UNIVERSITY OF CINCINNATI

Date: 04/27/2006

I, Kartikeya Mahalatkar,

hereby submit this work as part of the requirements for the degree of:

Master of Science

in:

Mechanical Engineering

It is entitled:

Cavitating Flow Over Oscillating Hydrofoils and Hydrofoil-Based Ship-Stabilization System

This work and its defense approved by:

Chair: Dr. Urmila Ghia

Dr. Karman Ghia

Dr. Rupak Banerjee

Cavitating Flow over Oscillating Hydrofoils and Hydrofoil-Based Ship Stabilization System

A dissertation submitted to the

Graduate School

of the University of Cincinnati

in partial fulfillment of the

requirements for the degree of

MASTER OF SCIENCE

in the Department of Mechanical, Industrial and Nuclear Engineering

Of the College of Engineering

By

KARTIKEYA KRISHNAJI MAHALATKAR

B.E., Mechanical Engineering

Veermata Jijabai Technological Institute, Mumbai University, June 2003

Committee Chair: Dr. Urmila Ghia

Abstract

Hydrofoils are used in maritime applications; such as ships and submarines, for stabilization, maneuvering, etc. In many of these applications, the hydrofoil may experience dynamic motion; an example would be an active-fin ship stabilization system where the hydrofoil oscillates periodically at large angles of attack. Computational Fluid Dynamics (CFD) is used for simulating the flow over an oscillating hydrofoil used in such systems. The CFD simulations for oscillating-hydrofoil flow are used in analysis of performance of the active-fin ship stabilization system. A system model has been created in MATLAB for this purpose. A Proportional Integral Derivative (PID) control system has also been developed to control the fin motion. Simulation of the active-fin ship-stabilization system in MATLAB provides the typical motion experienced by a hydrofoil used in ship stabilization. This motion is fed back to a CFD solver to determine the effect of non-sinusoidal oscillation on Lift, Drag and Moment of the hydrofoil. The aerodynamics of the non-sinusoidally oscillating hydrofoil is analyzed so as to find an optimum pitching motion for the hydrofoil so as to produce higher lift forces and thus provide better performance.

Another important aspect which affects the performance of an active-fin ship stabilization system is the cavitation occurring over the flow over oscillating hydrofoils. Cavitation occurs because the pressure on the suction side of the hydrofoil falls below the vapor pressure of water. Numerical simulations using Reynolds-averaged Navier-Stokes equations are carried out to analyze the effect of cavitation on the dynamic stall of an oscillating hydrofoil. It was found that the flow physics changes considerably with cavitation. The dynamic stall vortex (DSV) was formed at an angle of attack much smaller than that for the non-cavitating case. The vortical structures were found to be distorted as compared to the non-cavitating case. Cavitation led to large oscillations in coefficient of lift, drag and moment during the downward pitching motion and this can adversely affect the system.

Acknowledgements

First and foremost, I am grateful to my advisor Dr. Urmila Ghia and co-advisor Dr. Kirti "Karman" Ghia, for their continuous guidance and inspiration throughout the course of this research work. Their support and discussions have been critical to the success of this research. I would also like to thank Dr. Rupak Banerjee for reviewing my thesis and agreeing to be on the defense committee. I would like to specially thank my colleagues Suman Mishra, Jeff Litzler, Shirdish Poondru, Arun Prakash Raghupathy, Devkinandan Tokekar, Amit Kasliwal, Valentina Kaloyanova, Aravind Prakash and Arvind Kishore for their help at various times.

Sincere thanks to my Parents Dr. B. Y Krishnoji Rao and Prema Rao and my Sister Kripa Rao, for their constant motivation, affection and support while I have been away from home.

Table of Contents

List of Figures

Nomenclature

Ac = Area on Cap side For Hydraulic actuator

Ar = Area on Rod side for Hydraulic Circuit

a2 = Average wave slope considering length upto bilge keels

B = Maximum beam

Be = Bulk modulus of oil used in Hydraulic circuit

C = Damping coefficient for ship roll

Cc = Critical Damping =2(I+Io) n

Cp = Pressure coefficient

c = Chord length

dt = Time step

f = Mass fraction of vapor

GM = Metacentric Height

I = Inertia of ship

Io = Added Inertia because of water

k_g = Radius of gyration of ship

Kq1 = Flow rate through pump per mA current flow through servo valve

Ks = Linearized constant for Moment on ship for any angle of fin angle

Subcripts

k = turbulent kinetic energy

k* = reduced frequency

L = Ship length

Re = Reynolds number based on chord length

t = Time

t^* = Non-dimensional time

T = Time-period of hydrofoil oscillation

U = Free stream velocity

x = Distance along longitudinal axis of ship

i = Current supplied to the servo valve

V = Total volume of supply line + Volume of Hydraulic actuator

α = Instantaneous angle of attack

α_o = Mean angle of attack

$\Delta\alpha$ = Maximum change in angle of attack from the mean value

α_g = Volume fraction of non-condensable gas

α_v = Volume fraction of vapor phase

ε = Turbulent kinetic energy dissipation

ρ = Density of mixture phase (vapor + liquid)

ρ_l = Density of liquid phase

ρ_v = Density of vapor phase

σ = Cavitation number

ω = Angular velocity

ω_n = Natural Frequency of Ship roll

ξ = Damping Ratio

Δ = Weight of Ship

Chapter 1 Introduction

Active-fin sip-stabilizers are used in wide variety of ships to achieve roll stabilization. In this type of system, the hydrofoil oscillates periodically through large angles of attack. This type of roll stabilization systems is extensively used in ships to achieve stabilization and improved performance. In applications like the ship stabilizer, a large angle of attack is used to take advantage of the high lift force generated during the formation of dynamic stall vortex on the suction side of the hydrofoil.

Many researchers have studied dynamic stall of an airfoil oscillating at large angles of attack both experimentally and numerically. The high lift force generated by large angle of attack oscillating hydrofoil is because of two reasons. One reason is the delay in separation due to stabilizing effects brought about by motion of the hydrofoil. The second reason is the formation of vortex near the leading edge on the suction side of the hydrofoil and the increasing strength of this vortex as it moves downstream. The delay in separation and formation of dynamic stall vortex both depends on the motion of the hydrofoil and hence change in motion will greatly affect the lift force. The phenomenon of dynamic stall is crucial in the design of transport craft applications. In case of aerial rotor craft applications, dynamic stall adversely affects the performance as it results in oscillations in lift force generated, leading to difficulty in controlling the motion of the vehicle. In these types of motion, a sinusoidal motion can very accurately represent the oscillation of hydrofoil. Therefore, most studies on pitching airfoils/hydrofoils assume the motion to be sinusoidal, whereas the motion of hydrofoils

in a ship stabilization system will, in general, be non-sinusoidal. This can significantly alter the lift force generated by the hydrofoil.

Many researchers have worked on improving the control system design for active-fin ship stabilization system to bring about improvement in performance. Different types of control methods have been used to achieve improved performance even under off-design conditions. Some of the methods, which have been used, include Proportional, Integral, Derivative (PID) controller, adaptive linear quadratic compensator, and Neuro Fuzzy Intelligent control. Also, advanced control system design techniques such as the H-INFINITY control system design technique have been applied to design and optimize these control systems.

Although control system design can be optimized to achieve better system performance, another important aspect that can be used for enhancing the performance is improving the aerodynamics of the pitching hydrofoil to generate higher lift force using smaller size hydrofoils, thus reducing the weight and space occupied by the system.

To the best knowledge of the author, the aerodynamics of a hydrofoil with a non-sinusoidal oscillating motion similar to that encountered in a ship stabilization system has not been studied so far. In the present paper, we will be analyzing the aerodynamics of pitching hydrofoil, and use it to find the optimum pitching motion for the hydrofoil.

To simulate the motion of the hydrofoil, a mathematical model has been developed which includes the model for sea waves, ship roll, hydraulic circuit, mechanical actuator, fin dynamics, ship dynamics and control system. This mathematical model is solved in MATLAB SIMULINK, and provides the variation of the angle of attack of the hydrofoil with respect to time.

The non-uniform hydrofoil motion resulting from the model is used as input for CFD simulations using Reynolds-Averaged Navier-Stokes equations (RANS). The CFD tool used for the analysis is FLUENT. Validation studies have been carried out using sinusoidal hydrofoil motion at frequencies encountered by hydrofoils in ship stabilization systems and good comparisons have been obtained with experimental results. In the present study, the flow physics of the non-sinusoidally oscillating hydrofoil will be analyzed to find the optimum motion for the hydrofoil to generate maximum lift force, and develop better control strategies for the motion of the hydrofoil.

Another important phenomenon affecting the performance of hydrofoils in active-fin ship stabilization systems is that of cavitation. Cavitation is not a passive agent, and actively changes the flow physics over hydrofoils used in maritime applications, such as in ships and submarines for stabilization, maneuvering, etc. Previous research on cavitation has found that the presence of cavitation can modify the Strouhal number for vortex formation, and also the translational velocity of the vortex. Also, it has been found that the presence of a few microscopic bubbles at low void fraction could shift and macroscopically deform the structure of the vortex.

In many of the applications involving cavitating hydrofoils, the hydrofoil may also experience dynamic motion, such as in an active fin ship-stabilization system where the hydrofoil oscillates periodically through large angles of attack. Most of the research in the area of dynamic stall has been carried out for aerial rotor craft applications and hence does not involve the effect of cavitation on the vortical flow structure. On the other hand, for underwater applications such as active-fin ship-stabilization systems cavitation will occur in regions where the pressure falls below the vapor pressure. The presence of cavitation will affect the vortical flow structures and result in loss in performance. It is therefore necessary to understand the flow physics of cavitation occurring over an oscillating hydrofoil.

One of the objectives of the present study is to analyze the effects of cavitation on the vortex dynamics of a hydrofoil oscillating at large angles of attack. Coefficients of lift and drag are examined to understand how the flow physics is affected due to cavitation and hydrofoil oscillation.

1 .1 Motivation

Active-fin ship stabilization is a novel concept, and is now being studied by many researchers world-wide. The active-fin ship stabilization system is used in a wide variety of ships, to achieve effective roll reduction. It increases the comfort level of passengers on board, as well as enhances the performance of many of the systems onboard. Because of the various advantages offered by active-fin ship stabilization, research related to them is very important. Presently, much research is going on in the field of developing better control strategies for active-fin ship stabilization which will provide improved

performance even under very adverse sea conditions. However, the aerodynamics of the hydrofoil have not been examined in these efforts. One way to improve the aerodynamics of hydrofoil is to find the optimum pitch motion which will deliver large lift force and hence increased performance. Also, to the best knowledge of the author, the effect of cavitation on the flow physics of a large angle of attack oscillating hydrofoil have not been studied so far. Cavitation is likely to considerably modify the flow over oscillating hydrofoils. Numerical simulation is a useful tool in understanding the flow over oscillating hydrofoils, and gives good insight into the effect of hydrofoil motion on the lift force as well as effect of cavitation on the flow physics. The complete flow process cannot be quantified by experiments due to limitation in the design of measurement devices. In such cases, accurate numerical simulations provide in-depth understanding of the underlying physics of the problem at much reduced costs.

1 .2 Cavitation

Cavitation is a phenomenon which occurs due to the ambient pressure, p, falling below the vapor pressure p_V of the fluid. The value of p- p_V is called the tension, Δp, and the magnitude at which rupture occurs is the tensile strength of the liquid, Δp_c. Consider two molecules separated by a variable distance s.

Equilibrium occurs at a separation, where the intermolecular attractive forces given by are zero. If the intermolecular distance is increased then the attractive forces starts to increase and reaches a maximum at some distance x. Hence application of force equal to the intermolecular force at intermolecular distance x1 will completely rupture the fluid. In calculations are carried out based on the above principle than the amount of

force required to cause rupture in liquids will be very large, which is much higher than what is practically observed. This is because the tensile strength of a liquid is determined by weaknesses at points within the liquid. This weakness is caused by minute impurities and hence difficult to quantify.

In practical situations weakness can occur in two forms, one is due to the thermal motions of within liquid, which can result in microscopic voids that can cause the nuclei necessary for rupture, and growth of bubbles. The second form of weakness is because of small particles suspended in liquid.

There are various ways by which cavitation and its effect on the flow physics can be modeled using computational fluid dynamics. Section 2.2 covers the various research works, both experimental and numerical that have been carried out in this area.

1 .3 Active Fin Ship Stabilization

The basic working of Active-fin ship stabilization, its underlying concept, advantages and limitations are described in this section. An active-fin ship-stabilization system consists of oscillating fins that provide lift force such that the moment produced by these forces is in a direction counter to the roll motion of the ship. The fins are controlled usually by a Proportional, Integral and Derivate digital controller (PID) with precision electro-hydraulic servo valves and closed loop feedback. This basic control theory has been applied successfully in many ship stabilizer applications. The control system offers fully proportional and fully automatic sensing and actuation of the fin actuator assemblies, which results in smooth, exact stabilizer operation without objectionable dead band or lag. The control system infinitely adjusts the fin rotation to

exactly match the vessel's roll tendency, which ensures maximum roll reduction performance with minimum drag.

1.3.1 Advantages and Limitations

Active-Fin ship stabilization system is capable of providing more than 90% roll reduction during normal cruising conditions. This system, has several advantages over other roll stabilization systems such as bilge keels, anti rolling tanks and rudder roll damping systems as it optimizes stabilization performance and efficiency against cost, weight, power, space, and maintenance requirements.

However one major limitation of active-fin ship-stabilizer is that it does not have good performance at low speeds as the lift force generated by the fins decreases significantly.

1 .4 Organization of the Thesis

The present work is broadly organized into four other chapters. Chapter 2 describes the past research available in the literature and establishes the need for the present study. Chapter 3 provides the background on cavitation and the cavitation model used in the present study. Chapter 4 provides information on the system modeling of active-fin ship stabilization system. Chapter 5 presents the numerical methodology and turbulence model. Chapter 6 gives the results and discussion. Chapter 7 concludes the thesis by identifying important findings of the current study, and provides direction for future work.

Chapter 2 Literature Survey

This section highlights some of the research on dynamic stall, cavitation and active-fin ship stabilizer. Section 2.1 provides information on past studies on dynamic stall. Section 2.2 highlights the research carried out on cavitation including both the experimental and numerical simulations. Section 2.3 gives details on research in active-fin ship stabilization system. Finally section 2.4 gives the specific objectives we have met with the present research.

2 .1 Dynamic Stall Research

Dynamic stall is used to describe the delay in stall on wings and airfoils that are rapidly pitched beyond the static stall angle. There are various studies attempting to determine the response of rapid passage through the static stall angle. A considerable number of experimental investigations of airfoil dynamic stall including those by McCrosky (1981), Gangwani (1982) and Piziali (1983), Landon (1982) and Lorber (1991) are available. Favier et al (1992), have carried out dynamic stall experiments at complex motions. These measurements provide a database against which numerical methods can be calibrated and validated.

The early attempts to predict dynamic stall involved combined experimental-theoretical approach as outlined by Halfman (1951) et al. This approach was further developed by Ericsson and Reding (1976, 1979, 1984 and 1988). These methods gave a fairly good prediction of the dynamic stall lift overshoot. With the progress in

computational fluid dynamics numerical simulations of dynamic stall became a possibility. Early attempts in prediction of dynamic stall involved low Reynolds number laminar flow calculations. Laminar incompressible flow solutions over a modified NACA-0012 airfoil were obtained by Mehta (1977) using the vorticity-stream function formulation. Good qualitative agreement of the computations with water tunnel flow visualization was obtained and the development of the unsteady flow field and the loads were investigated. . Incompressible laminar dynamic stall flow fields were also investigated by Ghia et al. (1991, 1992) using the vorticity-stream function formulation. Again, favorable comparison of the computation with the smoke flow visualization was obtained. Dynamic stall of airfoils and wings in laminar flow is mainly of theoretical interest because fully laminar flow cannot be sustained at high Reynolds numbers which are observed in most applications.

Numerical investigations of dynamic stall in turbulent flow were conducted by Fung and Carr, (1991) who concluded that an increase of the reduced frequency delays the boundary layer separation and allows the airfoil to attain higher lift values at higher angles of attack. A problem encountered in several numerical investigations was lack of accuracy in the computation of dynamic stall hysteresis loops. Srinivasan et al. (1995) performed a systematic study of the effect of turbulence modeling on dynamic-stall computations in an attempt to improve the prediction of dynamic stall,. They used algebraic, half-equation and one-equation turbulence models.

One of the first numerical investigations of dynamic stall for compressible flow was presented by Sankar and Tassa, (1981). Compressible, unsteady, turbulent flow

computations were also obtained by Sankar and Tang (1985) and Rumsey and Anderson. (1988). The important contribution of these early investigations is that they have shown the ability of the numerical solutions to obtain certain flow field features similar to the available flow visualizations. The majority of the numerical work was directed towards the investigation and prediction of two-dimensional dynamic stall flow fields. Only recently, unsteady, three-dimensional flow fields, which are of primary interest in industrial applications, have been calculated for a pitching Newsome, R. W. (1994) and an oscillating wing Ekaterinaris, J. A. (1995).

Most of the research in the area of dynamic stall have been carried out for aerial rotorcraft applications and hence do not involve the affect of cavitation on the vortical flow structure. Whereas for underwater applications such as active-fin ship-stabilization systems cavitation will occur in regions where the pressure is below the vapor pressure The presence of cavitation will affect the vortical flow structures and result in loss in performance. It is therefore necessary to understand the flow physics of cavitation occurring over an oscillating hydrofoil.

2 .2 Cavitation Research

Cavitation is responsible for many undesirable effects and even damage in hydraulic installations such as in turbo machines or naval propellers. Various types of cavitation exist, including bubble cavitation, sheet cavitation, cloud cavitation, vortex cavitation.

Many authors in two main configurations, namely, Venturi- type sections and two dimensional foil sections, have studied cavitation experimentally. Venturi type sections

have been studied by Furness and Hutton (1975), Lush and Peters (1982), Stutz and Reboud (1997). Two dimensional foil sections have been studied by Kawanami et al. (1997), Pham et al. (1999), Arandt et al. (2000), Laberteaux and Ceccio (1998), and Astolfi et al (2001).

One of the important forms of cavitation is the cavitation on lifting surfaces. Hence the cavitation over two dimensional foil sections have been studied extensively. Kjeldsen, et al, (1999) have shown that a variety of cavitating flow patterns are possible within the sigma(cavitation number)-angle of attack plane. The sheet cavitation that occurs on the hydrofoil suction side has an unsteady behavior. This unsteady behavior has been attributed to the formation of a reentrant jet that flows under the cavity from its rear part to its upstream end and breaks of the cavity.

Although cavitating flow has several complex features, substantial efforts have been made in modeling cavitating flow. Most of the models are based on a single fluid approach i.e, relative motion between liquid and vapor phase are neglected and the liquid vapor mixture is treated as a homogeneous medium with variable density. Delannoy and Kueny (1990), Song and He (1998) and Merkle et al., related mixture density to the local void fraction by a state law. Kubota et al.(1992), Chen and Heister (1994) and Singhal et al. (2002), found mixture density by a supplementary equation relating the void fraction to the dynamic evolution of the bubble cluster. Kunz et al., calculated mixture density by developing a mass transfer law between liquid and vapor. The main numerical difficulties are the presence of strong compressibility of the two phase medium with quasi

incompressible behavior of the pure liquid flow and the influence of turbulence on the unsteady two phase flow.

Coutier-Delgosha et al. (2001) have carried out numerical studies using the RNG k-e turbulence model for cavitation over stationary hydrofoils. They found that the results obtained with RNG k-e model were in poor agreement with experimental results. The vapor cloud shedding was not captured, and a stable cavitation sheet was obtained instead. They attributed this to the over-prediction of eddy viscosity in regions of flow with high vapor concentration, and suggested a modification for the calculation of eddy viscosity. This modification to the turbulence model as suggested by Coutier-Delgosha is results in good agreement of the numerical simulations with experimental results.

Although the effect of cavitation over stationary foils has been studied extensively both experimentally and numerically, work on the effect of cavitation over oscillating hydrofoils has been very limited. Carron et al. (2000), studied the effect of flow unsteadiness on cavitation by using hydrofoils oscillating at small angles of attack and amplitude of oscillation. Cavitation over hydrofoils, oscillating at large angle of attacks that are above the static stall angle involves complex vortical flow structures. Although cavitation in vortical structures is a common problem in engineering applications, it has not been given extensive treatment. Examples of vortical flow structures in which cavitation can occur range from eddies that are randomly distributed in space and time in turbulent flows to well defined and relatively stable vortices found in propeller tips, in clearances of turbo machinery and on hydrofoils. Belahadji et al. (1995) have

experimentally studied the effect of cavitation on vortical flow structures in the wake of a wedge section. They found that cavitation modifies the Strouhal number for vortex formation, and also affects the translational velocity of the vortex. Xing et al. (2002), carried out numerical simulations of vortex cavitation in a three dimensional submerged transitional jet. They found that cavitation occurred in the core of the primary vortical structures, distorting and breaking up the vortex ring into several sections. Also, the velocity and transverse vorticity in the cavitating regions were intensified due to vapor formation, while the stream wise vorticity was weakened. Sridhar and Katz (1999) examined the effect of entrained bubbles on the structure of a vortex ring, and showed that the presence of a few microscopic bubbles at low void fraction could shift and macroscopically deform the structure of the vortex.

In the present study we have analyzed the effect of cavitation on complex vortical flow structure over oscillating hydrofoils.

2 .3 Active-Fin Ship Stabilization

Presently much of the research on Active-fin ship stabilization has been on improving the design of control system. Many researchers have worked on improving the control system design for active-fin ship stabilization system to bring about improvement in performance. Fortuna and Giovanni (1996), have used the adaptive linear quadratic compensator, Hickey et al. (1997), have used the H-INFINITY control system design technique to optimize controller design and Guo and Sun (1996) have applied Neuro Fuzzy Intelligent Control to achieve better system performance. Although control system design can be optimized to achieve better system performance another important aspect

that can be used for enhancing the performance is improving the aerodynamics of the pitching hydrofoil to generate higher lift force using smaller size hydrofoil thus reducing the weight and space occupied by the system.

2 .4 Specific Objectives

The objective of the present study is to analyze the effects of cavitation on the vortex dynamics of a hydrofoil oscillating at large angles of attack. Coefficients of lift and drag are examined to understand how the flow physics is affected due to cavitation and oscillating motion.

To the best knowledge of the authors, the aerodynamics of a hydrofoil with a non-sinusoidal oscillating motion similar to that encountered in a ship stabilization system has not been studied so far. In the present paper we will be analyzing the aerodynamics of pitching hydrofoil and use it to find the optimum pitching motion for the hydrofoil.

To simulate the motion of hydrofoil a mathematical model has been developed which includes the model for sea waves, ship roll, hydraulic circuit, mechanical actuator, fin dynamics, ship dynamics and control system. This mathematical model is solved in MATLAB SIMULINK, and provides the angle of attack of the hydrofoil with respect to time.

The aforementioned result for the non-uniform hydrofoil motion from the model will be used as an input for CFD simulations using Reynolds Averaged Navier Stokes equations (RANS). The CFD tool used for the analysis is FLUENT. Validation studies

have been carried out using sinusoidal motion at frequencies encountered by hydrofoil in ship stabilization systems and good comparisons have been obtained with experimental results. In the present study, the flow physics of the non-sinusoidally oscillating hydrofoil will be analyzed to find the optimum motion for the hydrofoil to generate maximum lift force and develop better control strategies for the motion of the hydrofoil.

Chapter 3 System Modeling of Active Fin Ship Stabilization

In this Chapter, we discuss the mathematical models developed for sea waves, ship roll, hydraulic circuit, fin dynamics and ship dynamics. A PID control system has also been developed to control the fin motion.

3 .1 Modeling of Sea Waves

Ocean Waves are seldom regular, but they can be modeled as a composition of regular waves. Regular waves are simple sinusoidal waves with varying amplitudes an frequencies. Superimposing sinusoidal waves of different wavelengths and heights on each other generates an irregular wave pattern (Ref. [10]). This irregular wave is used for finding out the effect of waves on the ship hull. The irregular sea wave obtained should have approximately the same significant wave height and mean wave period as that assumed for generating it.

The Power Density Spectrum (PDS) was used to obtain the wavelengths and amplitudes of the simple regular waves. The equation for the PDS as specified by International Towing Tank Conference is given as,

$$S(\omega) = \frac{172.75 H_{1/3}^2}{T^4 \omega^5} e^{\left(\frac{-691}{T^4 \omega^4}\right)} \tag{3.1}$$

This is a two-parameter spectrum, used to simulate fully developed seas with infinite depth. Thus, for generating the power spectrum the significant wave height and mean

time period are assumed. The PDS is representative of the total energy of the sea per square meter of sea surface. The energy of the sea wave at any frequency is proportional to the square of the amplitude of the waves coming at that frequency.

Then at any particular frequency 'ω' we can find the amplitude of regular wave as,

$$S(\omega)\Delta\omega = 1/2\sum \zeta^2 \tag{3.2}$$

Where, ζ is the amplitude of waves at frequency ω

or,

$$\zeta_\omega = \sqrt{2S(\omega)\Delta\omega} \tag{3.3}$$

By taking small value of Δω, a large number of regular waves at different frequency is generated. The summation of the motion of these regular waves gives the simulation of the sea wave. The resultant sea wave obtained is found to have a significant wave height and average time period reasonably close to what was assumed in the PDS equation.

Reference [9] gives the probability of getting waves of particular mean time period and significant wave height for world seas and Atlantic ocean. At any particular wave height the mean time period is selected for maximum probability of occurrence.

3 .2 Mathematical Modeling of Ship Roll Using Simple Linear Theory of Rolling

The roll of the ship is found by calculating the torque effect of buoyancy forces due to simple sinusoidal waves. The procedure for determining the frequency, amplitude and wavelength of these sinusoidal waves was shown above. The resulting roll motion is obtained by superimposing the roll motions due to these individual sinusoidal waves. Connolly [11], has developed a linear mathematical model for simulating response due to simple sinusoidal waves. Connolly assumed that a simplified form having constant draught represents the ship hull and has sections, which are wall-sided at the water line where the width is b (Fig. 4). The waterline width itself is assumed to be varying in a parabolic manner given by the equation.

$$\frac{b}{B} = 1 - \left(\frac{2x}{L}\right)^2 \tag{3.4}$$

where, B = maximum beam

L = Ship length

x = Distance along longitudinal axis of ship

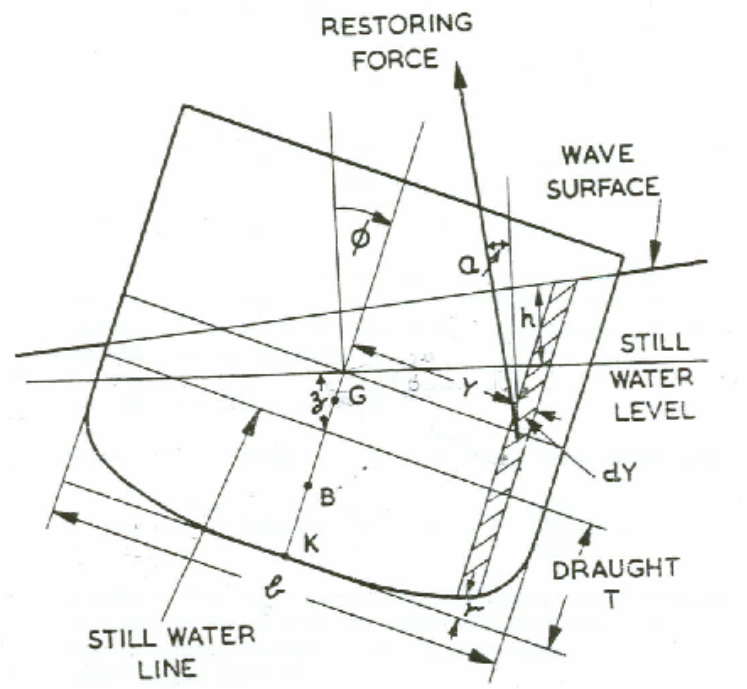

Fig 3.1: Restoring Force on a rolling ship due to buoyancy effects.

Assuming the above profile for the ship, the roll due to sinusoidal waves can be calculated as,

$$(I + Io)\ddot{\phi} + C\dot{\phi} + \overline{GM}\ \Delta\phi = -(Io\ddot{a}_2 + Ca_2 + \overline{GM}\ \Delta a_1) \qquad (3.5)$$

This model is solved in MATLAB to obtain the ship roll motion due to irregular sea waves.

3 .3 Model of Hydraulic Circuit and Actuator for Stabilizer System

The exact details of Hydraulic circuit designed by Larsen and Toubro Ltd are company confidential and therefore cannot be provided. The figure below shows the hydraulic circuits for a typical hydro steering system, the cylinders at the top of the figure are the hydraulic actuator similar to those used for controlling the fin motion in present system.

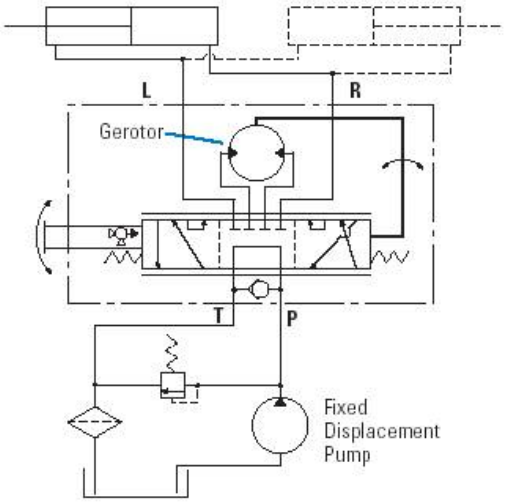

Fig 3.2 Hydraulic Circuit for a typical hydro steering system

Appropriate mathematical models have been developed for each of the components involved in the hydraulic circuit including pump, servo valve, accumulators, hydraulic actuators etc.

3 .4 Fin or Hydrofoil Dynamics

The hydrodynamic force on the hydrofoil is found by assuming a sinusoidal pitch motion for the hydrofoil at the mean time period of hydrofoil motion. The coefficient of Lift and hydrodynamic moment coefficient is shown in the figure below.

A straight line fit is assumed for the lift force in the simulation as shown in the figure. A fourth order polynomial is used for approximating the Hydrodynamic moment coefficient of the hydrofoil.

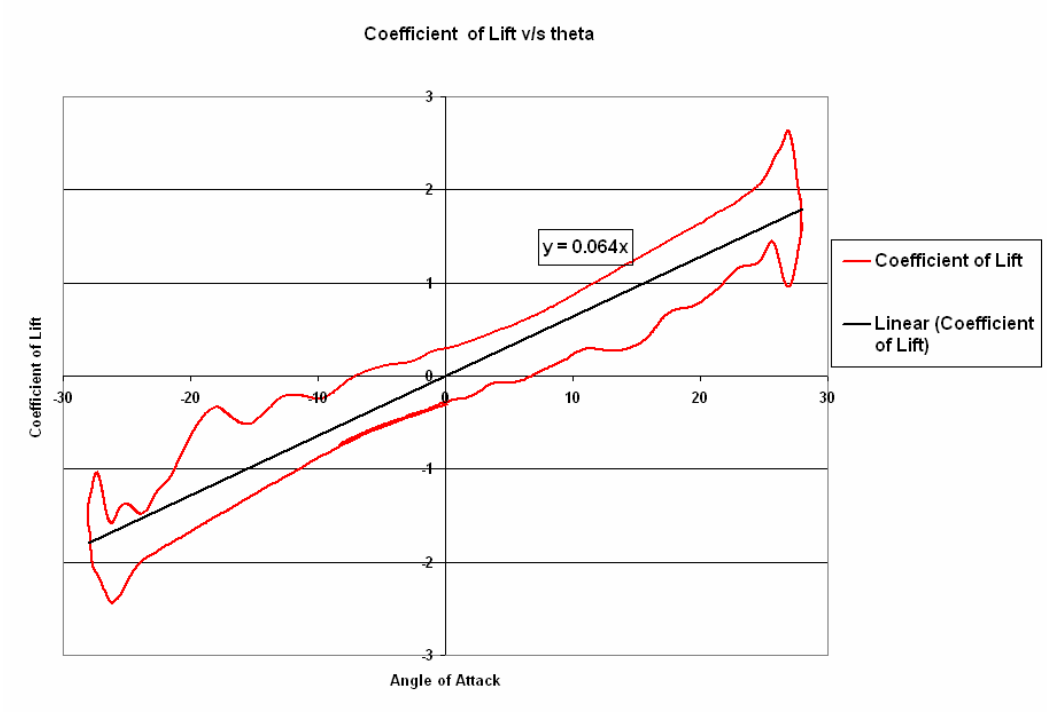

Fig 3.2 Coefficient of Lift vs Angle of Attack, $\alpha_m = 0^o$, $\Delta\ \alpha = 28^o$, Re= 10^6.

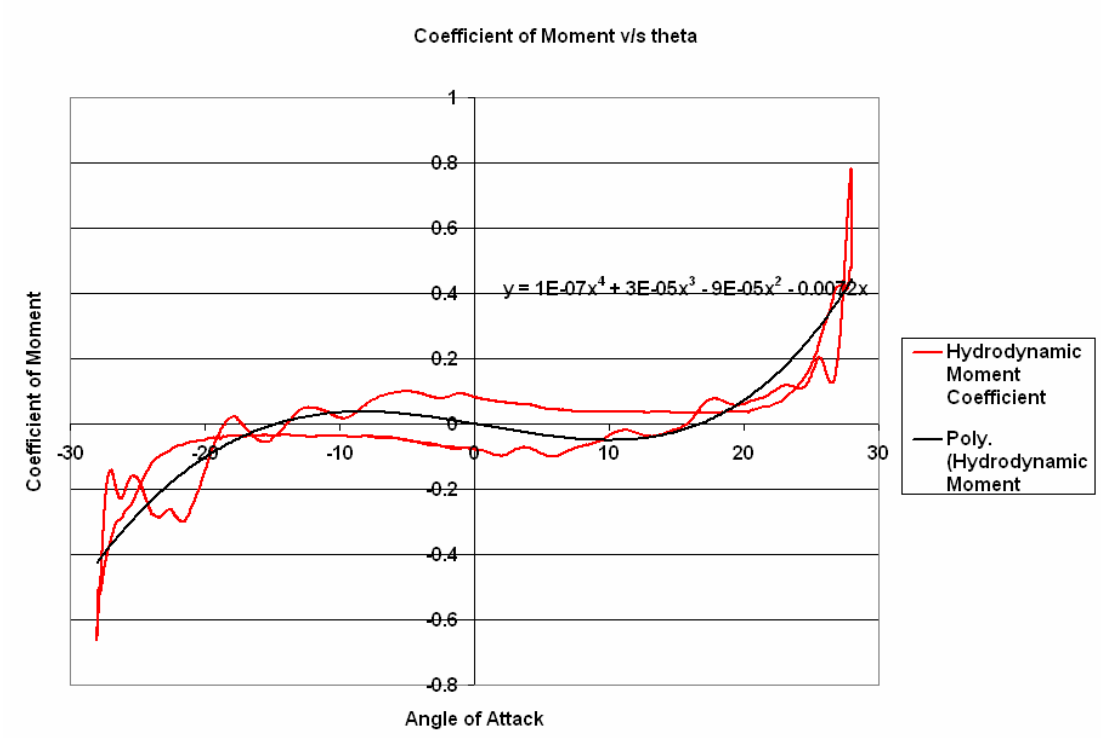

Fig 3.3 Coefficient of Drag vs Angle of Attack, αm = 0^o, Δa = 28^o, Re= 10^6.

The equation for fin-dynamics can be given as

$$I_F \overset{oo}{\theta} + T_{Friction}(\overset{o}{\theta}) = T_{Hydrodynamic} + T_{HydraulicCircuit} \quad (3.6)$$

$T_{HydraulicCircuit}$ = **Torque exerted by the hydraulic actuator on the Hydrofoils**

$T_{Hydrodynamic}$ = **Torque due to hydrodynamic forces acting on the Hydrofoils**

3 .5 Mathematical Model of Ship

The ship roll motion can be given a second order linear differential equation given below

$$(I + Io)\overset{oo}{\phi} + 2N\overset{o}{\phi} + \overline{GM}\,\Delta\phi = stabilizer\_moment \quad (3.7)$$

It is a second order linear differential equation

Where, Stabilizer moment = Lift force x Distance of Fin from center of gravity of Ship

3 .6 System Structure and Transfer Function

The active-fin ship stabilization system can be represented by a block diagram as shown in figure below. Connolly's model for ship roll described above is used for calculating the ship roll angle, roll velocity and roll acceleration when no stabilization is present. The counter roll angle, roll velocity and roll acceleration produced by the active-fin ship stabilizer is calculated using the system model described earlier. The difference between roll motion when no stabilization is present and the roll produced by the stabilizer gives the net or actual roll experienced by the ship and is fed as an input to the control system, which controls a hydraulic circuit operating an actuator controlling the motion of hydrofoil. The motion of hydrofoil determines the lift force and hydrodynamic

moment on the hydrofoils which are approximated by assuming appropriate equations as mentioned in the section of Fin/Hydrofoil dynamics. Knowing the lift force generated by the fin the response of the ship due to stabilization system can be ascertained.

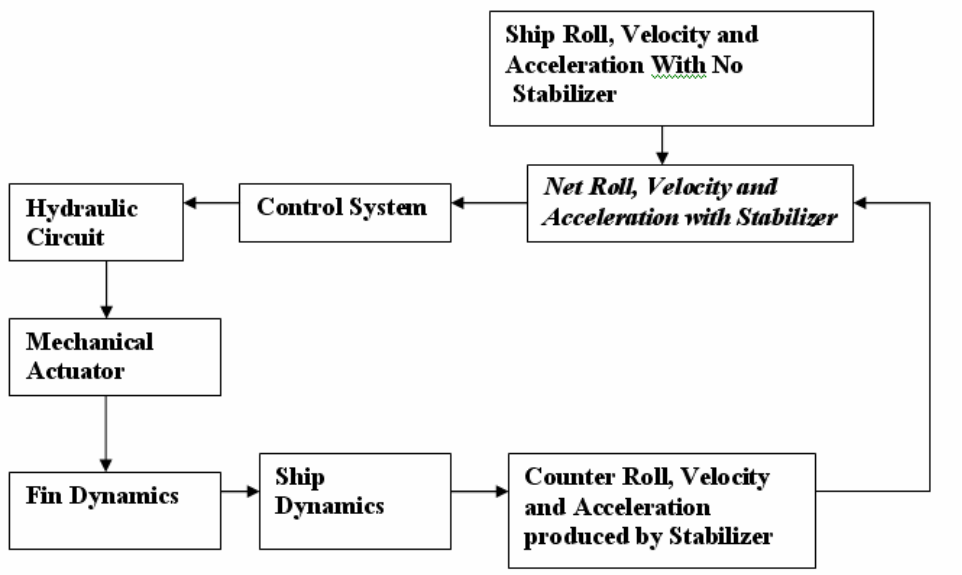

Fig 3.4 Block Diagram for Active-Fin Ship-Stabilization System

The open loop transfer function can be deduced from the mathematical models developed for individual systems mentioned above and is given by the equation below.

$$\frac{\theta(s)}{i(s)} = \frac{Ks}{\left((I + I_0)s^2 + Cs + \Delta.g.GM.\right)} \times \frac{Kq1}{Ts+1} \times \frac{\left(\frac{2K_{q1}}{Ts+1}\right)(A_C + A_R).r}{\frac{sV_O}{B_E}\left(s^2 I_F + K_F\right) + 2rs(A_C + A_R)(A_C + A_R).r} \qquad (3.8)$$

Where,

i = Current input from control system to the pump of hydraulic circuit

T = Ship roll due to stabilizer

A PID Control system was used in this system but the details of the control system is of proprietary nature to Larsen and Toubro Ltd. A broad outline of the requirements is given

below. The stabilizer system is to be capable of correcting the roll effectively at maximum significant wave height of 5.5m, at ship speed of 18 knots. The system is to be designed for $+28^{o}$ travel of the fins at normal cruising speed of 18 knots and $+18^{o}$ at maximum speed of 33 knots. The stabilizer system should be able to develop a total lift force of approximately 700 KN at a cruising speed of 18 knots. The fin area is chosen so as to provide sufficient lift force. This is based on the ship specifications. It is desired that at the design conditions specified amount of stabilization is obtained from the system.

Chapter 4 Numerical Methodology

This chapter describes the Turbulence model and Validation methodology followed to study the flow physics over stationary/oscillating hydrofoil with/without cavitation. The geometry, governing equation, and boundary conditions are first described.

4 .1 Governing Equations

The single fluid approach is used for the analysis of cavitation. In the single fluid approach the phases are assumed to be interpenetrating mixture. It is assumed that there are no relative velocities between the two phases i.e. the model is a homogeneous multiphase model. In the single fluid approach we solve the continuity equation for the mixture, the momentum equation for the mixture, and the volume fraction equation for the secondary phases.

$$\frac{\partial}{\partial t}(\rho_m) + \nabla.(\rho_m \vec{V_m}) = R_e - R_c \tag{4.1}$$

where, ρ_m is the mixture density and Vm is given as

$$\vec{V_m} = \frac{\sum \alpha_k \rho_k \vec{v_k}}{\rho_m} \tag{4.2}$$

α_k is the volume fraction of phase k.

The momentum equation for the mixture can be obtained by summing the individual momentum equations for all phases. It can be expressed as

where, $\frac{\partial}{\partial t}\left(\rho_m \vec{v}_m\right)+\nabla.\left(\rho_m \vec{v}_m \vec{v}_m\right)=-\nabla p+\nabla.\left[\mu_m\left(\nabla\vec{v}_m+\nabla\vec{v}_m^{\,T}\right)\right]$ (4.3)

μ_m is the viscosity of the mixture and is given as

$$\mu_m=\sum \alpha_k \mu_k$$

4 .2 SIMPLE Algorithm

The Semi Implicit Pressure Linked Equation (SIMPLE) algorithm is widely used for solving the incompressible Navier-Stokes equation and is also used for solving the governing equations described above. It mainly consists of the following steps:

1) An approximation of the velocity field is obtained by solving the momentum equation by assuming the pressure gradient term is calculated using the pressure distribution from the previous iteration or an initial guess

2) The pressure equation is formulated and solved in order to obtain the new pressure distribution.

3) Velocities are corrected and a new set of conservative fluxes are calculated.

4 .3 Geometry, Grid, and Boundary Conditions

Both NACA 0015 and NACA 0012 profiles were used in the present analysis. This was because the dyanamic stall phenomena has been studied extensively for the NACA 0012 profile whereas NACA 0015 has been used extensively in analyzing cavitation over hydrofoils. The commercial software Fluent v6.2 was used for the present

simulations, because of its ability to carry out cavitation analysis and simulate dynamic motion of bodies. A dynamic, unstructured grid, with remeshing and smoothing, was used for simulating the oscillating hydrofoil. The upstream was located at 10 chord lengths from the trailing edge and downstream at 20 chord lengths. The number of cells in the domain was 0.2 million. The upstream boundary condition was set as constant velocity, and at downstream, a constant pressure boundary condition was used.

4 .4 Cavitation Modeling

The full cavitation model developed by Singhal et al. (2002) is used in the present simulations. This model takes into account all first order effects in cavitation model. This model involves two phases (liquid and vapor) and a certain fraction of non-condensable gases, whose mass fraction is known in advance. Non-condensable gas is seen to considerably modify the flow physics. This model takes into account the formation and collapse of the bubbles.

4.4.1 Numerical Formulation of Cavitation model avitation Modeling

The full cavitation model developed by Singhal et al. (2002) is used in the present simulations. This model takes into account all first order effects in cavitation model. This model involves two phases (liquid and vapor) and a certain fraction of non-condensable gases, whose mass fraction is known in advance. Non condensable gas is seen to considerably modify the flow physics. This model takes into account the formation and collapse of the bubbles.

The numerical model is based on the Reynolds Averaged Navier-Stokes equations as well as a conventional turbulence model (for example, standard k-epsilon model or

RNG k-epsilon model). The working fluid is assumed to be a mixture of three species (liquid, vapour and non-condensable gas). The mass fraction, f, affects to the fluid density and its governing equation is:

$$\frac{\partial}{\partial t}(\rho f) + \nabla \cdot (\rho \vec{V} f) = \nabla \cdot (\Gamma \nabla f) + R_e - R_c \tag{4.4}$$

The source terms Re and Rc represent vapour generation and collapse rates, which can be a function of the main flow parameters. In fact, the expressions used in this cavitation model are functions of the static pressure and are given by these two equations (4.5) and (4.6). Non-condensable gas evolved during the presence of cavitation has been considered in these equations.

$$R_e = C_e \frac{\sqrt{k}}{\sigma} \rho_l \rho_v \sqrt{\frac{2(\rho_v - \rho)}{3\rho_l}} (1 - f_v - f_g) \tag{4.5}$$

$$R_c = C_c \frac{\sqrt{k}}{\sigma} \rho_l \rho_l \sqrt{\frac{2(\rho - \rho_v)}{3\rho_l}} f_v \tag{4.6}$$

FLUENT V6.2 cavitation model allows the use of a slip velocity between the bubbles and the liquid. However, in all the models used in present work, this slip velocity has not been considered.

4 .5 Turbulence Modeling

Turbulence model is one of the key elements in Computational Fluid Dynamics (CFD). It is important that the turbulence model chosen is capable of accurately capturing

the essence of the relevant physics. For each of the problems analyzed validation studies have been carried out to see if the chosen turbulence model is able to capture the flow physics accurately. Different turbulence models have been used depending on the case and have been described below.

4.5.1 Cavitation over Stationary Hydrofoil

The RNG k-epsilon turbulence model was used because of availability of suitable damping functions for accurate simulation of cavitation. The Reynolds number of the flow was 10^5, and a y+ of around 1 was used for the first point off the surface.

Coutier-Delgosha et al. (2001) have carried out numerical studies using the RNG k-ε turbulence model for cavitation over stationary hydrofoils. They found that the results obtained with RNG k-ε model were in poor agreement with experimental results. The vapor cloud shedding was not captured, and a stable cavitation sheet was obtained instead. They attributed this to the over-prediction of eddy viscosity in regions of flow with high vapor concentration, and suggested a modification for the calculation of eddy viscosity based on the equation given below.

$$\mu_t = f(\rho) C_\mu \frac{k^2}{\varepsilon} \tag{4.7}$$

where,

$$f(\rho) = \rho_v + \left(\frac{\rho_v - \rho}{\rho_v - \rho_l} \right)^n (\rho_l - \rho_v) \tag{4.8}$$

A value of n = 10 was suggested by the authors to obtain good agreement with the experimental results.

In the present analysis, a test case was run to simulate the oscillating hydrofoil with no cavitation using the RNG k-e model. The angle of attack was varying as a function of time based on the equation given below

$$a = a_o + \Delta a \sin(2k^* t^*) \tag{4.9}$$

t* = non-dimensional time = tU/c, k* = reduced frequency = $\frac{\omega c}{2U}$ and ω = angular velocity = $\frac{2\pi}{T}$. The following parameters were used in the simulation; k* = 0.15, a_o = 15^o, Δa = 10^o and Re = 10^6.

4.5.2 Cavitation over Oscillating Hydrofoil

Comparing the results from present simulation with numerical results of Guilmineau et al. (1997) and experimental results of Raffel et al. (1995), it was found that the separation occurred at the expected angle of attack, but the formation of secondary vortices was not captured and the strength of the primary vortex was considerably lower than expected. This was attributed to the high eddy viscosity in the core of the primary vortex. For a better comparison with the numerical and experimental results, the eddy viscosity was reduced to 40% of its original value and was given by equation (4.10).

$$\mu_t = AC_\mu \frac{k^2}{\varepsilon} \tag{4.10}$$

where A = 0.4.

For simulations with cavitation and oscillation of hydrofoil the modifications to turbulent eddy viscosity given by equations (4.7) and (4.10) were used and hence, the equation for turbulent eddy viscosity is given as,

$$\mu_t = A \times f(\rho) C_\mu \frac{k^2}{\varepsilon} \tag{4.11}$$

A better modification for the turbulent eddy viscosity in equation (4.11) could be a damping function based on pressure rather than a constant scaling factor. As the pressure is lower in the vortex core region, a function of pressure can be used for reducing the turbulent eddy viscosity in vortex core regions. This is being considered for future simulations.

4 .6 Validation Methodology

To the best knowledge of the authors, experimental or numerical work on large angle of attack oscillating hydrofoils with cavitation is not available. Hence, to validate the present simulations, a non-cavitating oscillating hydrofoil and a stationary hydrofoil with cavitation were considered. The table below shows the various validation studies carried out.

Table 4.1 Validation Cases to study Cavitation and Oscillating Hydrofoil

Case	Reference	Conditions	Quantities Compared
1	McAlister et al. (1982)	**Oscillating Hydrofoil No Cavitation,** Reduced Frequency=0.25, Mean angle of attack =15, Amplitude of Oscillation =10. Profile – NACA 0012 Reynolds Number = 10^6 Pitching Axis at Quarter Chord	• Coefficient of Lift • Coefficient of Drag
2	Arndt et al. (2000) and Qin et al. (2003).	**Stationary Hydrofoil With Cavitation** Angle of attack = 8, Cavitation number = 0.5-2.5 Profile – NACA 0015	• Mean Coefficient of Lift • Frequency of oscillation of cavity

4.6.1 Validation Study for Oscillating Hydrofoil without Cavitation

The simulation of sinusoidally oscillating hydrofoil was carried out to validate the dynamic mesh model in Fluent and a summary of the case conditions is shown in Table 4.1. A NACA-0012 profile was used for the validation study. The frequency of oscillation of the hydrofoil is defined by the non-dimensional parameter "reduced frequency", defined by

$$k = \frac{\pi c}{TU} \tag{4.12}$$

The formation of a dynamic stall vortex and other secondary and tertiary vortices were captured in the simulation. A good match with experimental data was obtained for the coefficient of lift and drag as shown in the Figures 4.1 and 4.2. The formation of

dynamic stall vortex was also predicted, and is primarily responsible for the large increase in lift force.

Figures 4.2 and 4.3 indicate reasonably good qualitative comparison between experimental data and the present simulations. A comparison of time averaged lift and drag values is shown in Table 4.2. For the validation study, simulations were carried out for four cycles, with the last cycle used for time averaging.

Table 4.2: Validation Studies and Comparison with Experimental results

Values	**Experimental (Time - Averaged over 50 cycles)**	**Numerical (Time Averaged over one-cycle)**	**Percentage Error of Numerical results in comparison to Experimental**
Lift	**1.135**	**1.140**	**0.5%**
Drag	**0.271**	**0.279**	**2.95%**

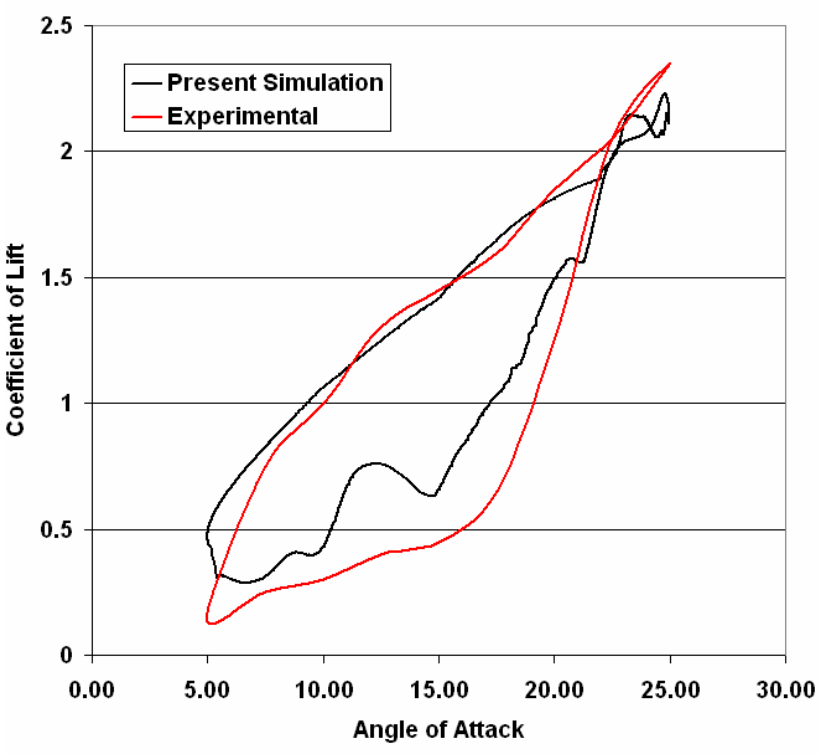

Fig. 4.1. Coefficient of Lift vs. Angle of Attack, Re = 10^6.

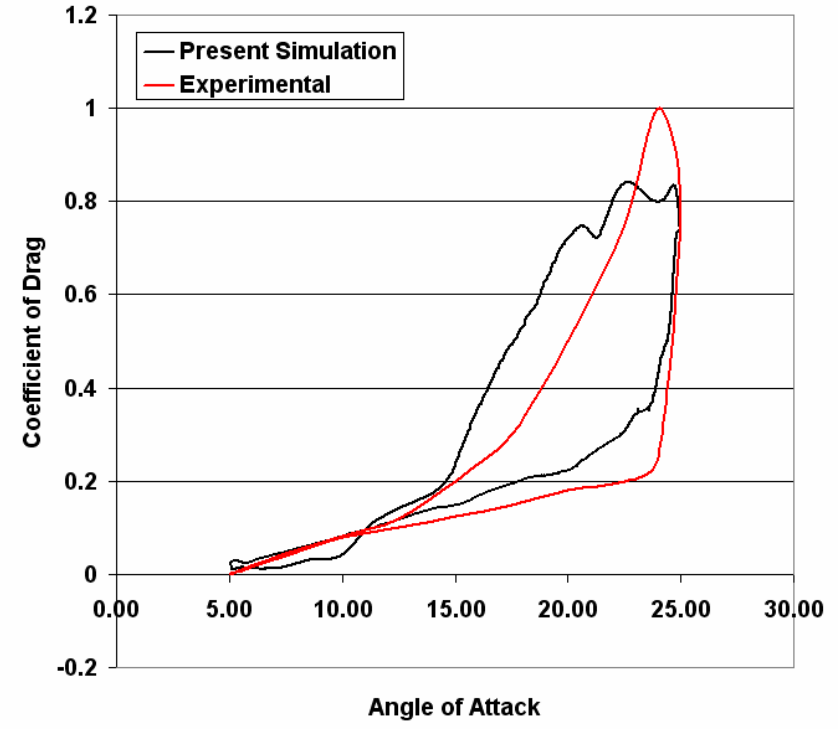

Fig. 4.2. Coefficient of Drag vs. Angle of Attack, Re =10^6.

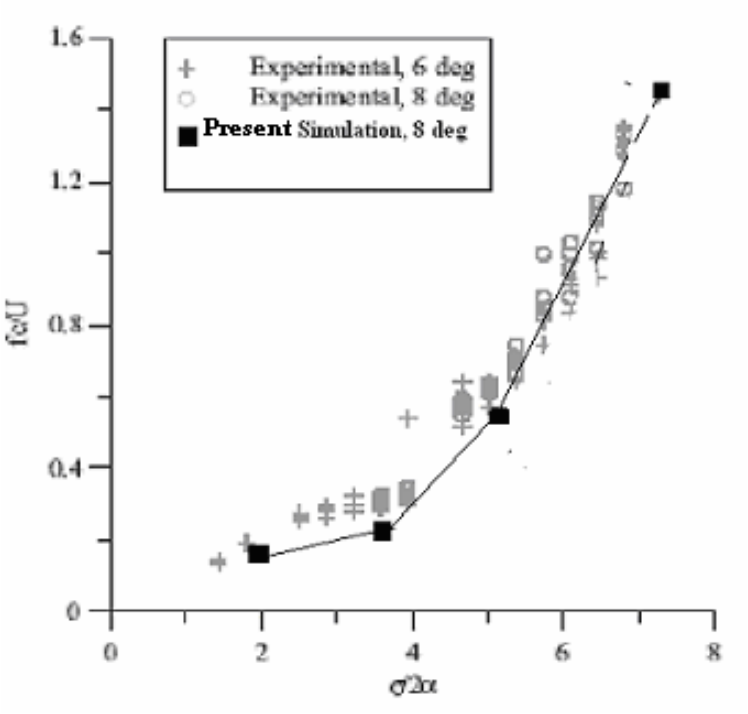

Fig. 4.3. Frequency of oscillation of sheet cavity, Re = 10^5.

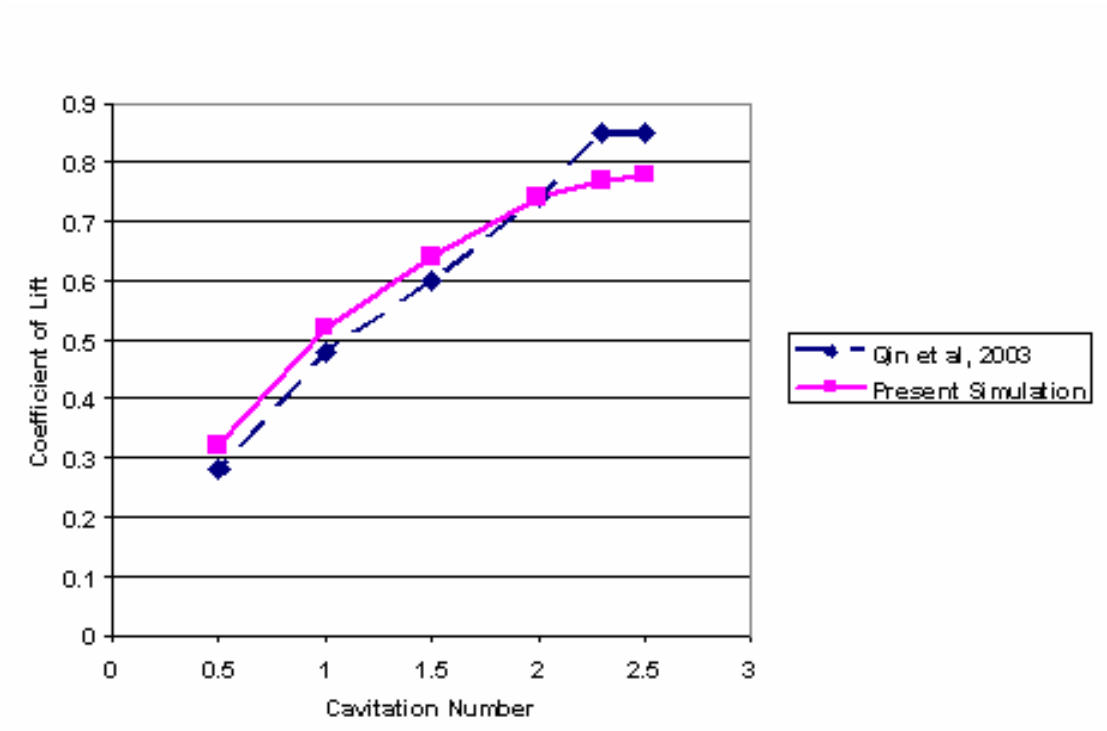

Fig. 4.4. Time-averaged coefficient of Lift, Re = 10^5.

4.6.2 Validation Study for Stationary Hydrofoil with Cavitation

The analysis was carried out at an angle of attack of 8 degrees, for cavitation numbers in the range 0.5 to 2.5, in order to simulate various cavitation flow regimes, and estimate the effect of cavitation on the lift force. Equation 4.7 was used to modify the turbulent eddy viscosity. A good match was obtained with the experimental results of Arndt et al. (2000) for the oscillation frequency of the cavitation sheet cavity. The time-averaged coefficient of lift also showed a reasonably good agreement with the numerical results of Qin et al. (2003).

Chapter 5 Results and Discussion

In this Chapter, Section 5.1 deals with the analysis of cavitating flow over oscillating hydrofoil. Section 5.2 provides the results for analysis of aerodynamics of hydrofoil for typical ship stabilization.

5 .1 Analysis of Cavitation over Oscillating Hydrofoil

The validation studies indicated good agreement of the numerical results for a stationary hydrofoil with cavitation and an oscillating hydrofoil experiencing no cavitation. Next, we use the cavitation model described in Section 4.4 to analyze the effects of cavitation on the flow over a dynamically oscillating hydrofoil. To understand the effect of cavitation on dynamic stall, the vortical flow structures in the cavitating and non-cavitating cases are analyzed. Finally, the behavior of the coefficient of lift is also studied as this is vital for a ship stabilization system.

5.1.1 Vortex Dynamics for Oscillating Hydrofoil without Cavitation

Figure 5.1 shows the sequence of events as the hydrofoil oscillates. The mainstream flow is at an angle of 15^o with respect to the horizontal. Figure 5.1a shows the hydrofoil at an angle of attack of 14.67^o, and pitching upwards. The flow is fully attached at this instant. The flow remains attached even as the hydrofoil pitches upwards, and crosses the static stall angle. Separation occurs at an angle of attack of around 21^o, starting near the trailing edge and moving towards the leading edge as the angle of attack is increased.

Figure 5.1b shows the flow at an angle of attack of 21.57^{o} and the separated flow can be clearly seen on the suction side of the hydrofoil. As the hydrofoil pitches up, a dynamic stall vortex (Vortex 'A') forms on the suction surface at an angle of attack between 22^{o}-23^{o} (Fig. 5.1c), and then convects downstream. Two other vortices, vortex 'B' and vortex 'C', are also formed near the leading edge. Vortex 'B' rotates in the counterclockwise direction and Vortex 'C' in the clockwise direction. The dynamic stall vortex is primarily responsible for the large rise in lift force, and is rotating in the clockwise direction. As the hydrofoil reaches the maximum angle of attack and starts pitching downward, the primary dynamic stall vortex gains strength and moves downstream (Fig. 5.1d). When the dynamic stall vortex reaches the trailing edge it interacts with the flow on the high pressure side and results in the formation of vortex 'D', which rotates in counterclockwise direction (Fig. 5.1e). The counterclockwise rotating vortices 'B' and 'D' merge. As, the hydrofoil pitches downward, the Vortex 'C' moves downstream, and the separation point starts to move towards the trailing edge as can be seen in Fig. 5.1f. The above discussion indicates the complex vortex structures existing during the dynamic stall phenomenon.

5.1.2 Vortex Dynamics for Oscillating Hydrofoil with Cavitation

The flow over an oscillating hydrofoil is significantly altered by the presence of cavitation. The cavitation number for the present analysis was taken as 2.7. This was based on the cavitation number experienced by a hydrofoil in the ship stabilization system. The dynamic stall vortex was formed at an angle 14^{o}-15^{o} (Fig 5.2a) in the cavitating flow as compared to an angle of, 22^{o}-23^{o} (Fig. 5.1c) in the non-cavitating case. This early formation of the dynamic stall vortex was attributed to expansion of the separation bubble, which exists near the suction peak of the hydrofoil, due to vapor

formation. Two vortices 'B' and 'C' are formed near the leading edge (Fig. 5.2b). Vortex 'B' is rotating in the clockwise direction, and Vortex 'C' is rotating in the counterclockwise direction. Cavitation occurs in the core of the vortex structures as this is a region of low pressure. Cavitation limits the minimum pressure in the core of the vortex to the vapor pressure. There is considerable difference in the vortical structure of the cavitating and non-cavitating cases. By comparing Fig. 5.1c for the non-cavitating case with Fig. 5.2c for the cavitating case, we can see that the dynamic stall vortex (Vortex 'A') is considerably distorted for the cavitating case. This can be attributed to expansion of vortex core due to vapor formation. As the dynamic stall vortex moves towards the trailing edge, it interacts with the flow on the high-pressure side, and results in the formation of the counter-rotating vortex 'D' near the trailing edge. This vortex is much weaker in the cavitating case as compared to the non-cavitating case. The pairing of vortices 'B' and 'D' which was observed in the non-cavitating case does not occur in the cavitating case, and this can be attributed to the lower strength of these vortices. Vortex 'C' is seen to gain considerable strength (Figs. 5.2d and 5.2e), and this was not observed in the non-cavitating case. This can be attributed to the early formation and passage of dynamic stall vortex, and other secondary and tertiary vortices such as 'B' and 'C'. Also observed is the formation of Vortices 'E' and 'F', in the cavitating case, causing further oscillation in the lift force as these vortices move downstream. Thus, the cavitation is not a passive agent and considerably modifies the vortex structure in the flow over an oscillating hydrofoil.

Figures 5.3a-5.3f show the phase contours at various angles of attack. Cavitation can be clearly seen in the core of the vortex structures, and causes its distortion. Figure. 5.3a shows the formation of cavity sheet at the leading edge, and also at the core of the dynamic stall vortex which is in its initial stages of formation. As the dynamic stall 1vortex gains strength, the size of the cavitation cloud in its core increases (Fig. 5.3b). Figure 5.3c shows the sudden inception of cavitation in vortex D. This creates oscillations in the lift force and may also produce much noise and vibration. The tertiary and quaternary vortices 'E' and 'F' also have considerable vapor formation in their cores. As the hydrofoil pitches downwards, the separation point starts moving towards the trailing edge. Figure 5.3 helps in the visualization of the formation, convection and dissipation of vapor clouds in the flow field.

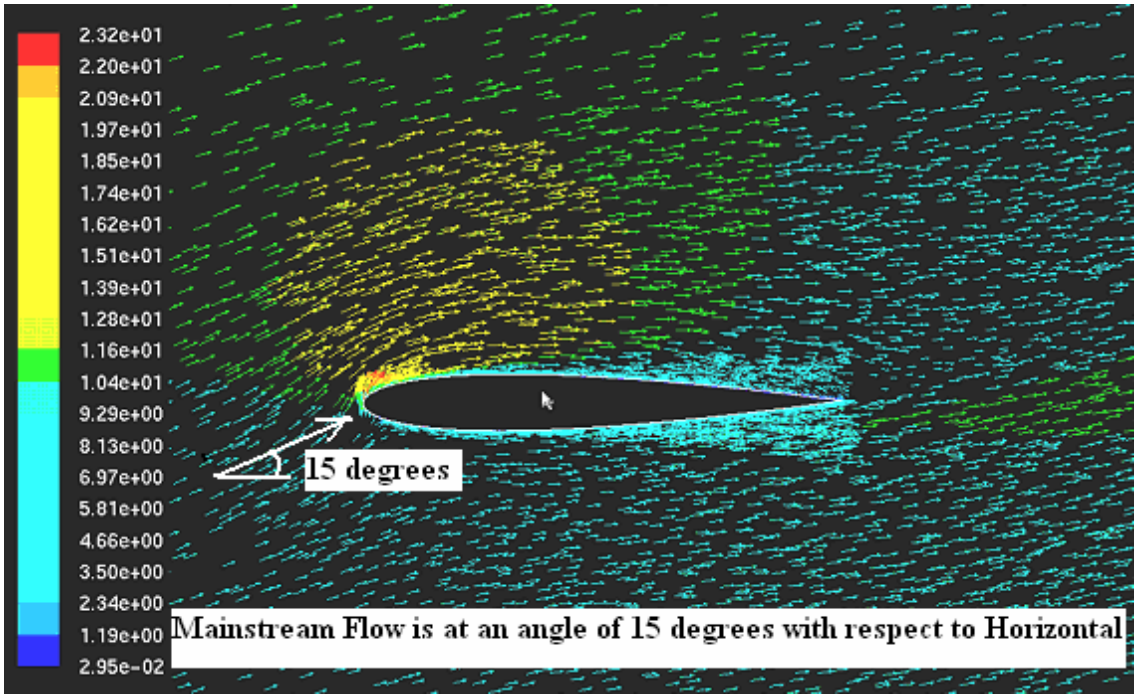

5.1a) Angle = 14.67^{o}

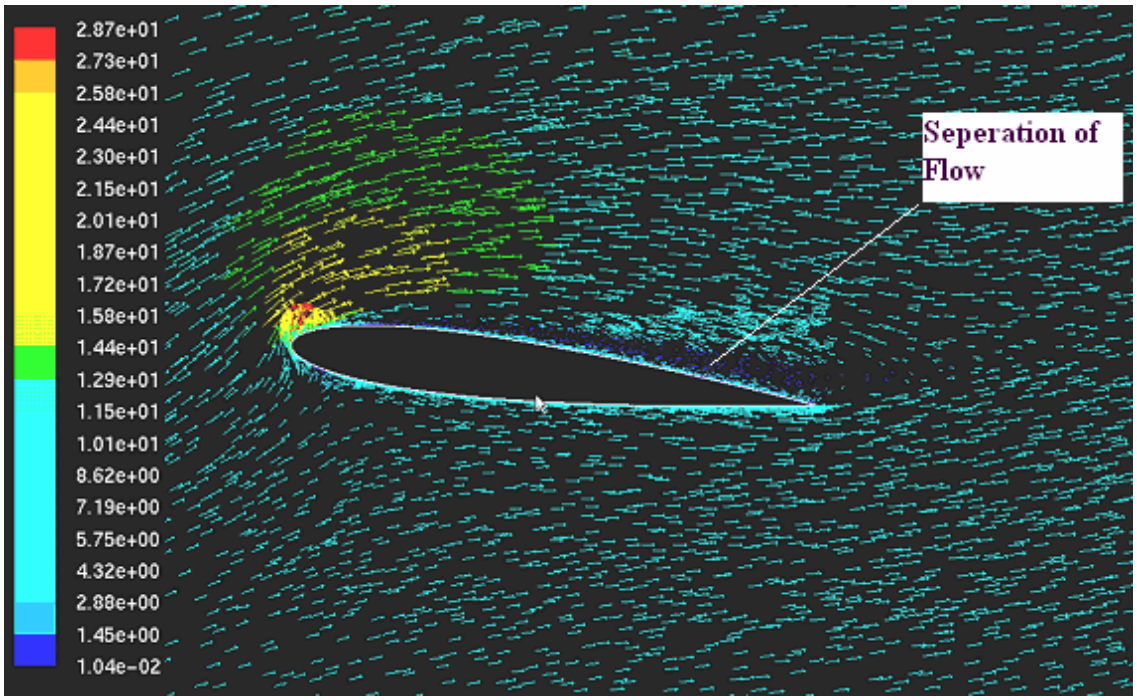

5.1b) Angle = 21.57^{o}

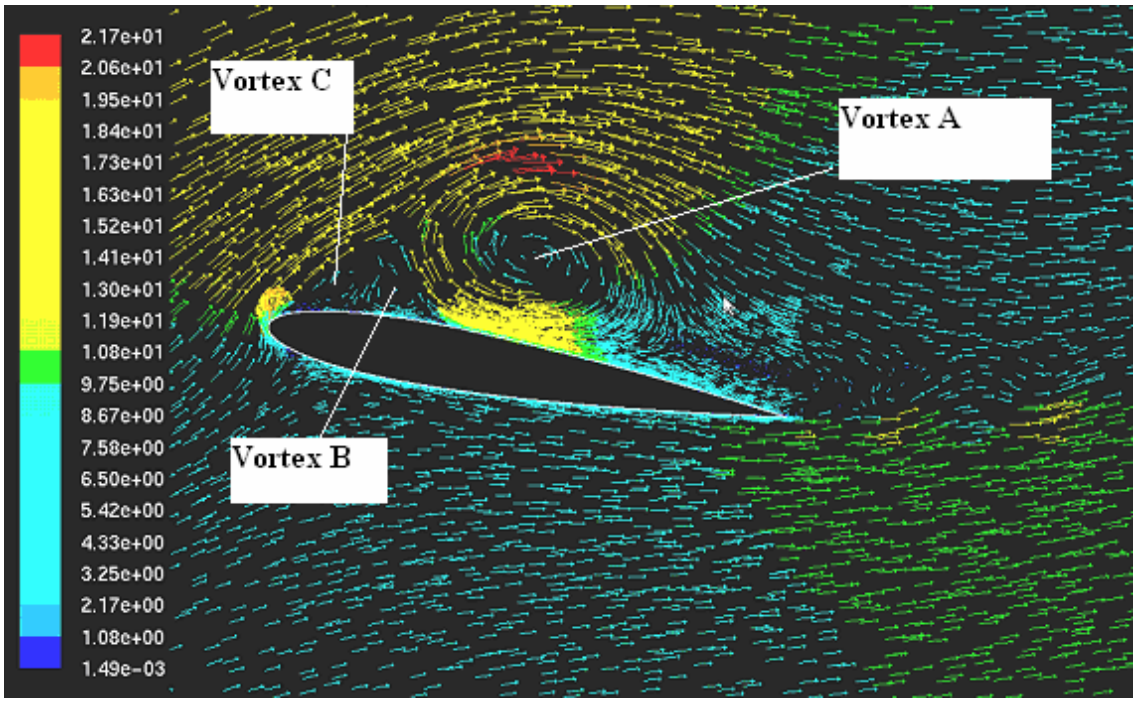

5.1c) Angle = 24.95^{o}

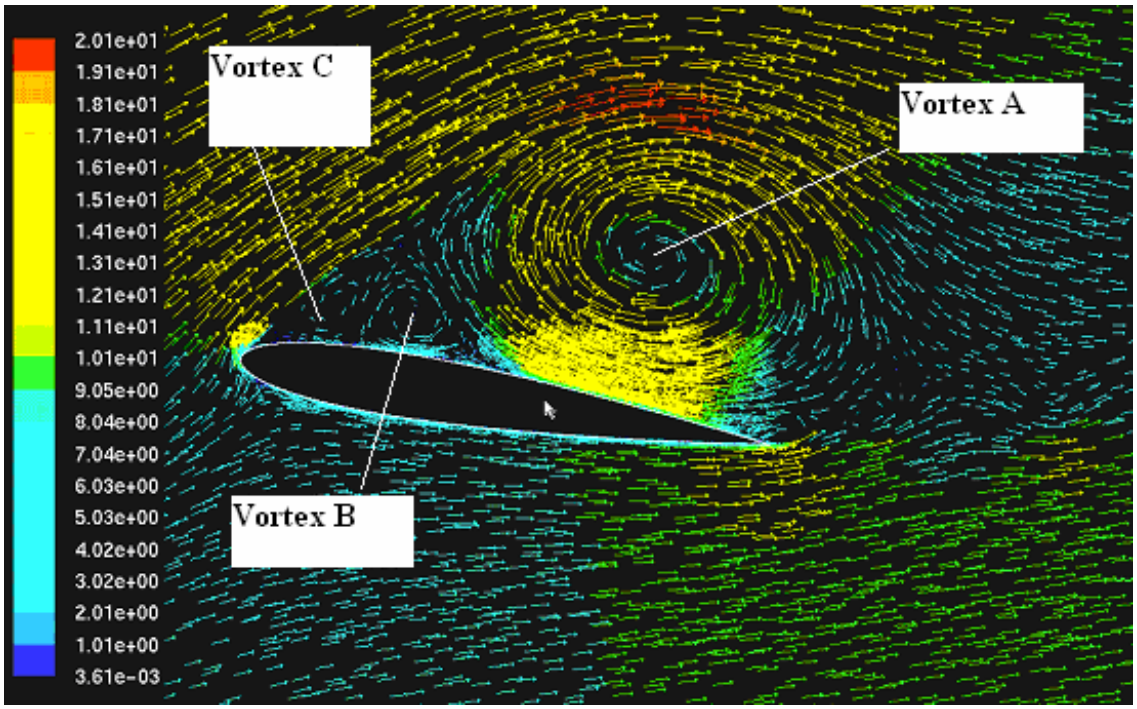

5.1d) Angle = 24.23^{o}

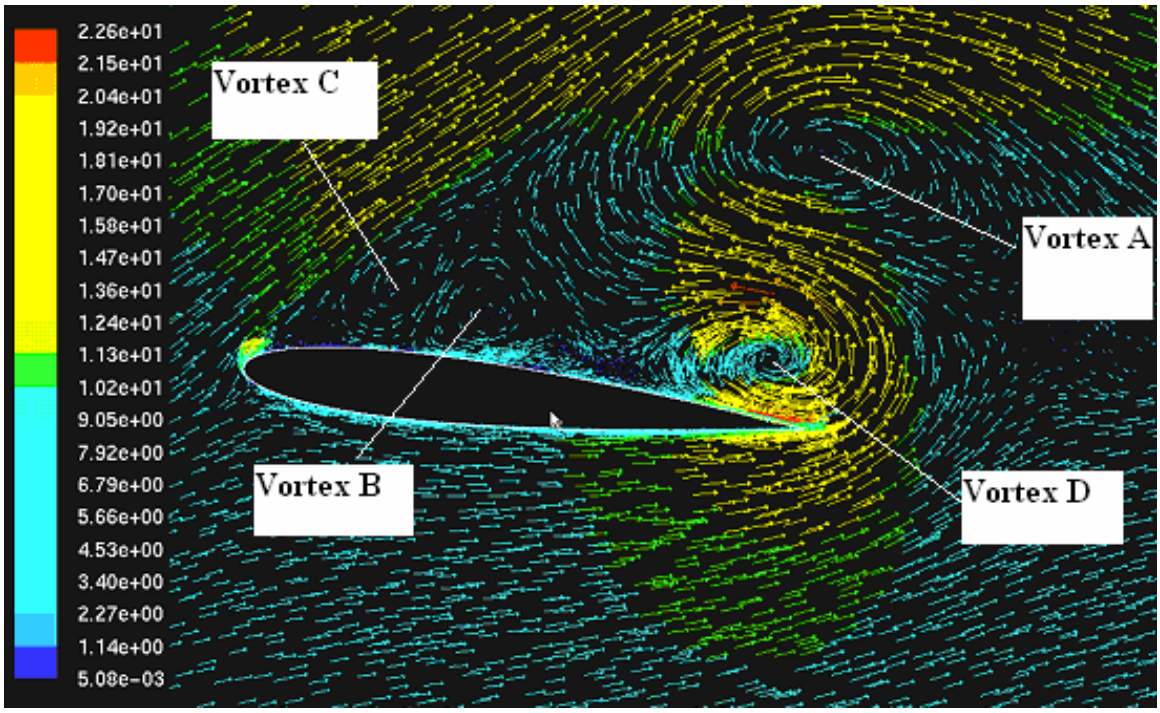

5.1e) Angle = 21.57^{o}

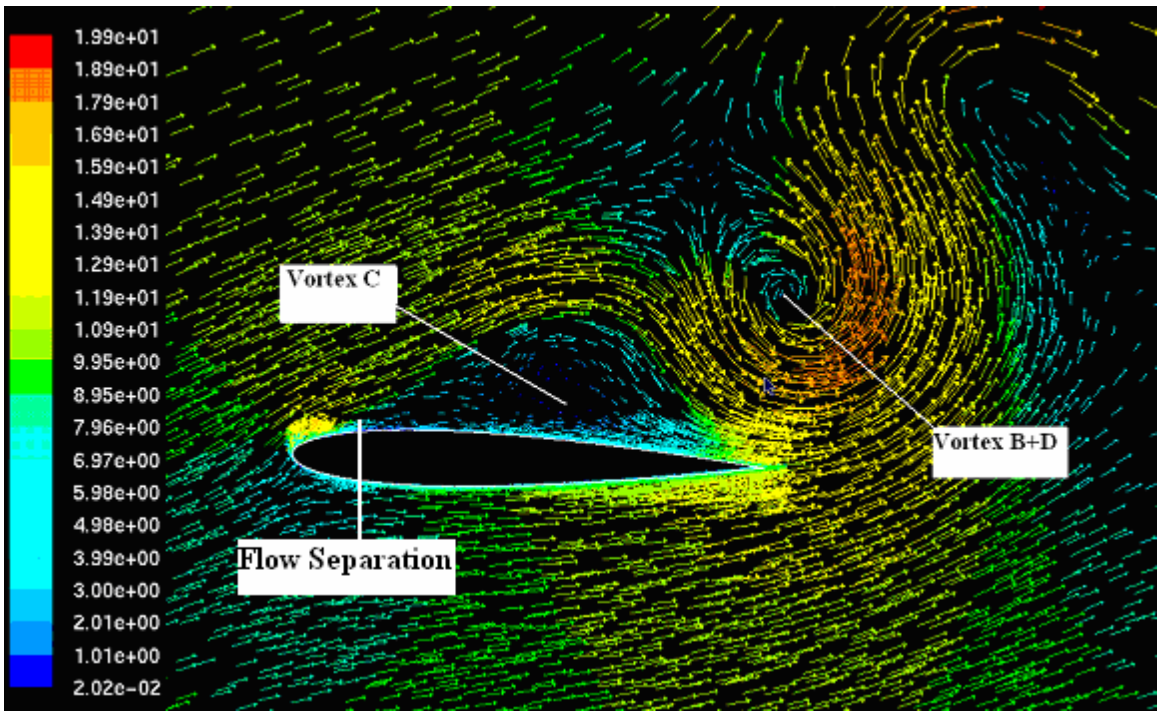

5.1f) Angle = 16.73^{o}

Fig 5.1 Velocity Vector for Oscillating Hydrofoil, k = 0.25, No Cavitation, Re = 10^{5}

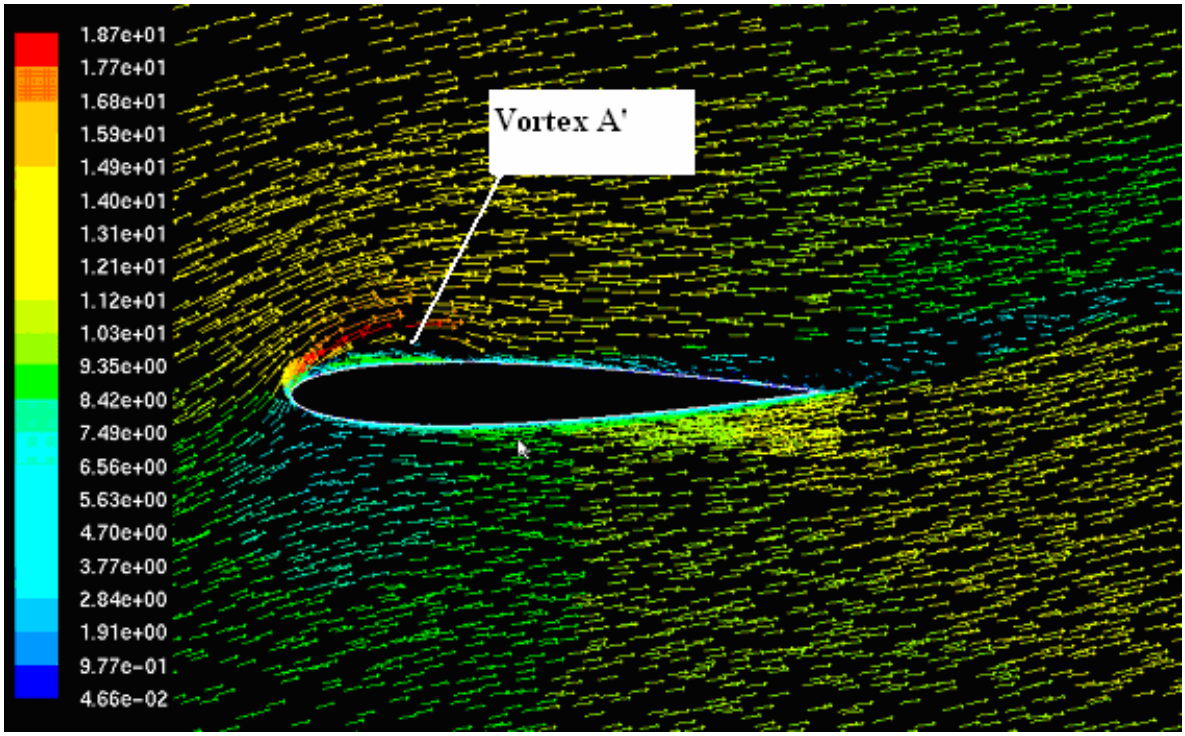

5.2a) Angle = 14.67^{o}

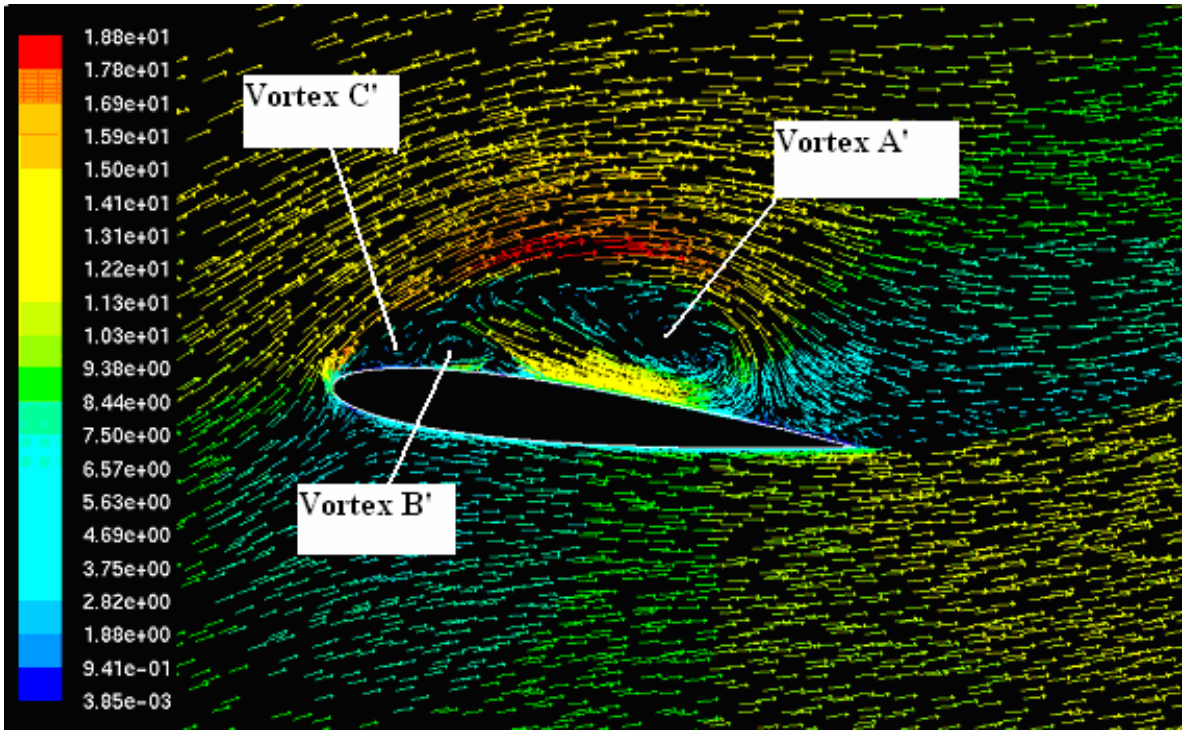

5.2b) Angle = 21.57^{o}

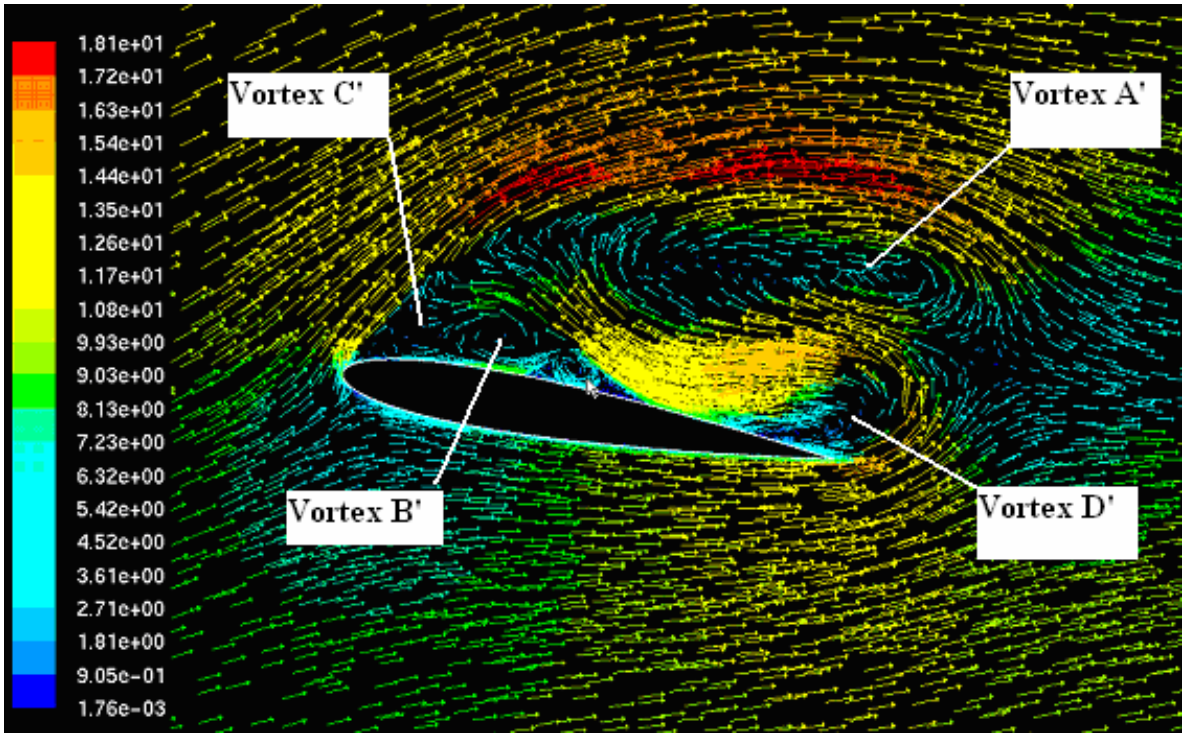

5.2c) Angle = 24.95^{o}

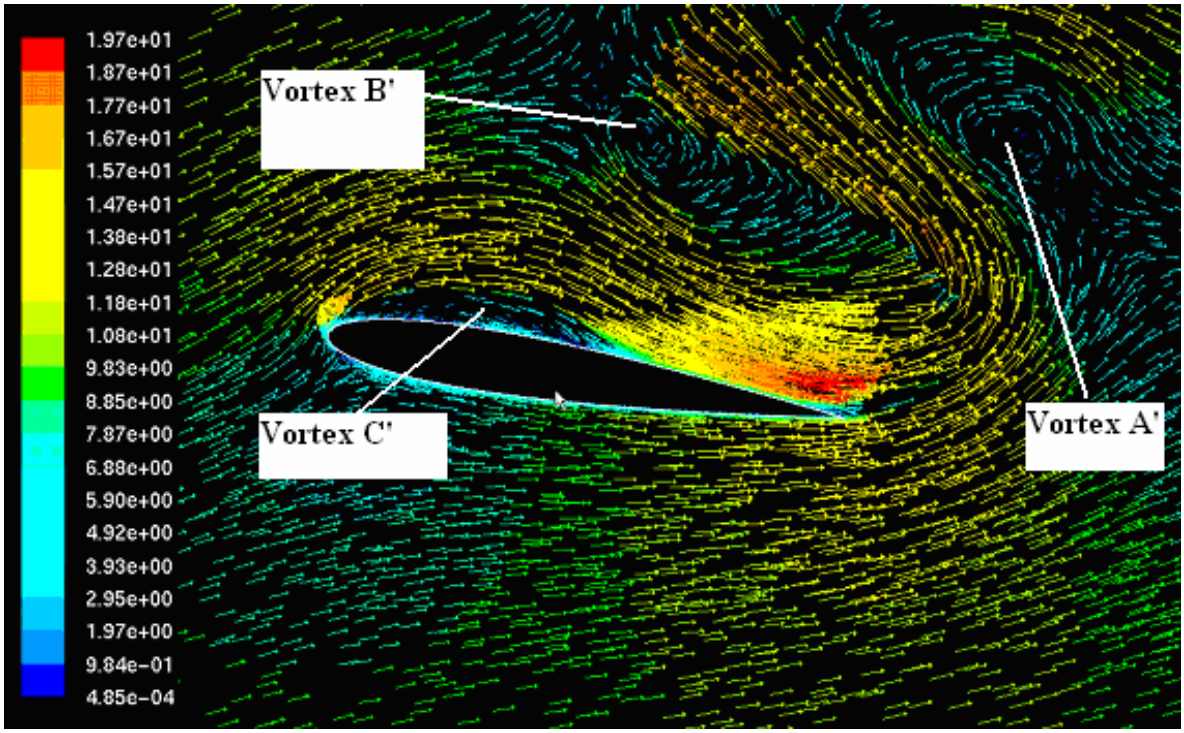

5.2d) Angle = 24.23^{o}

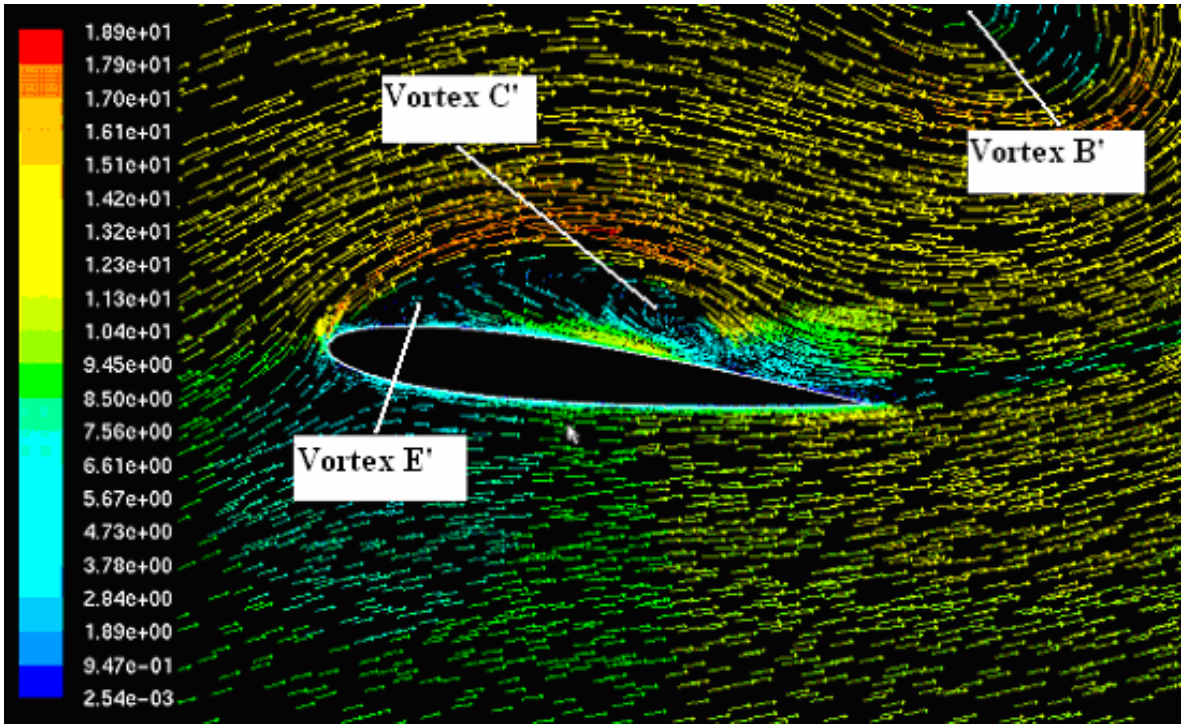

5.2e) Angle = 21.24^{o}

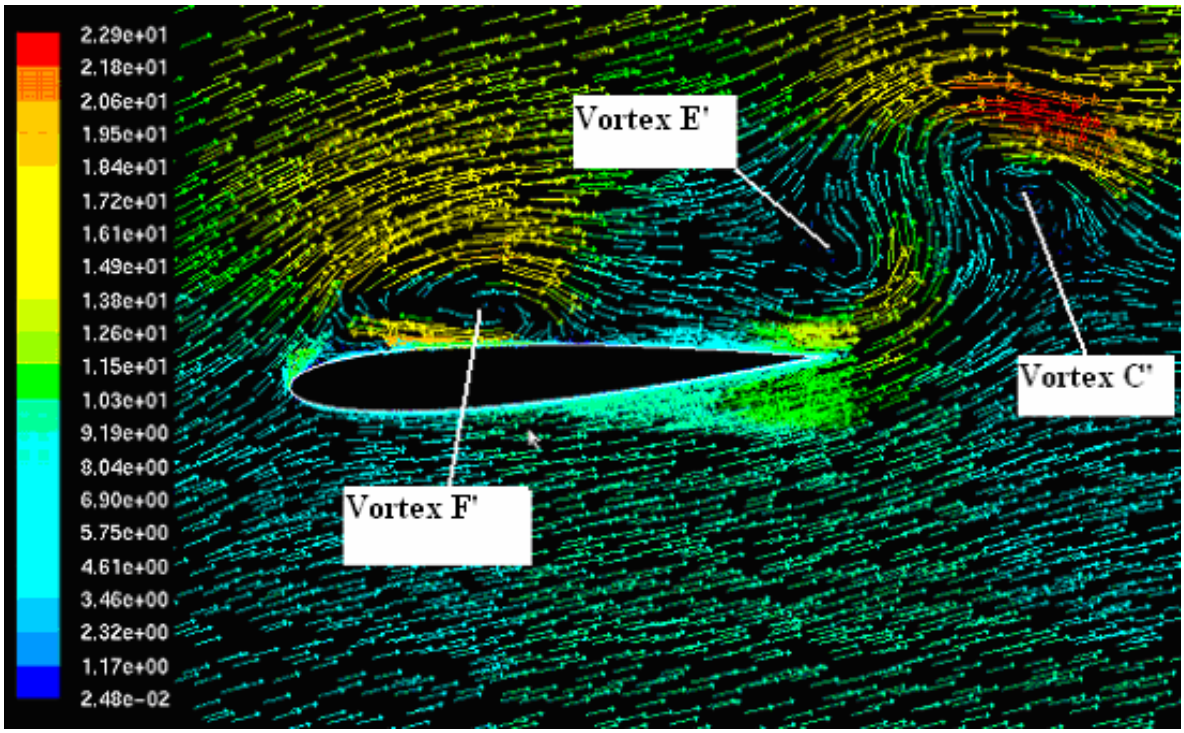

5.2f) Angle = 11.8^{o}

Fig 5.2 Velocity Vector for Oscillating Hydrofoil, k = 0.25, s = 2.7, Re = 10^{5}

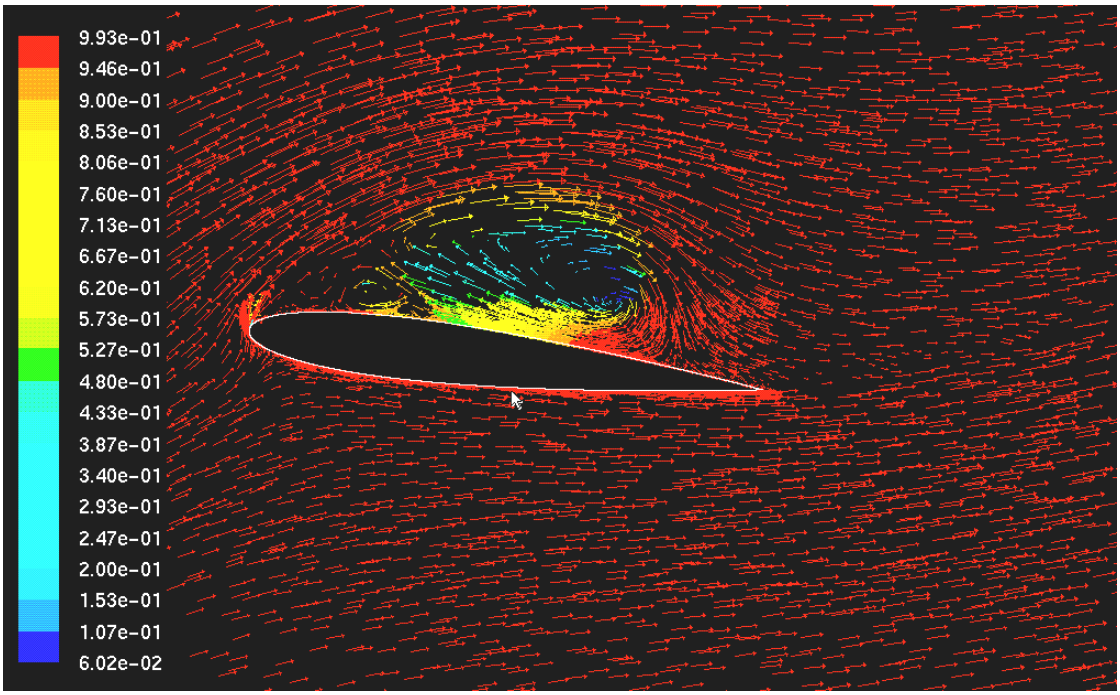

5.3 a) Angle = 14.67^{o}

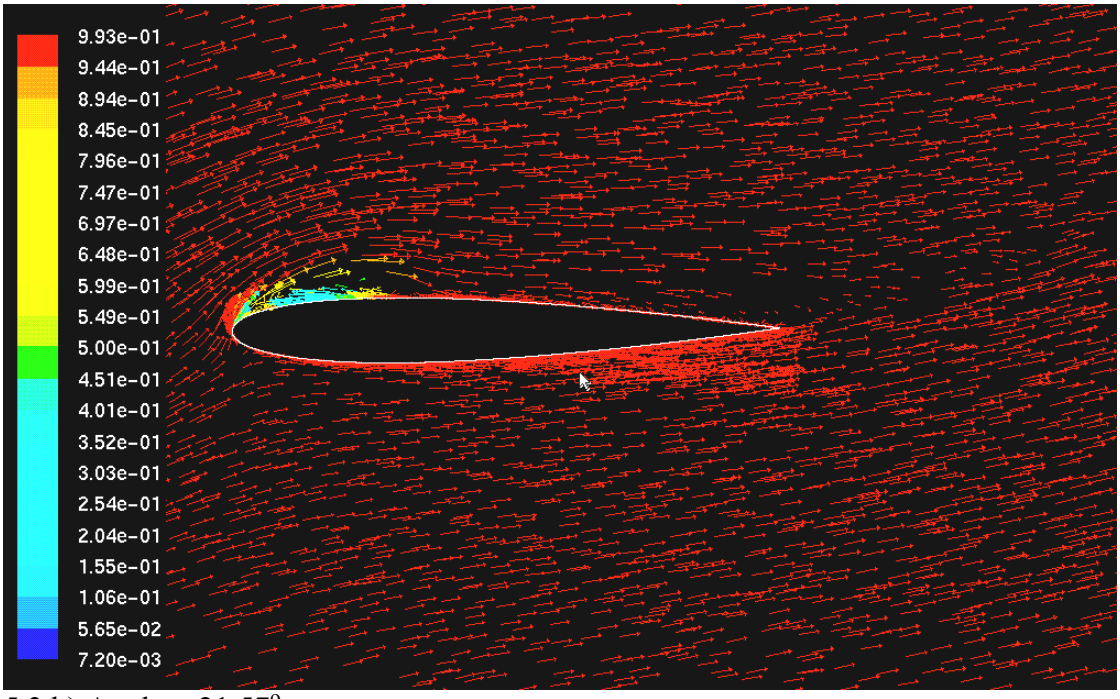

5.3 b) Angle = 21.57^{o}

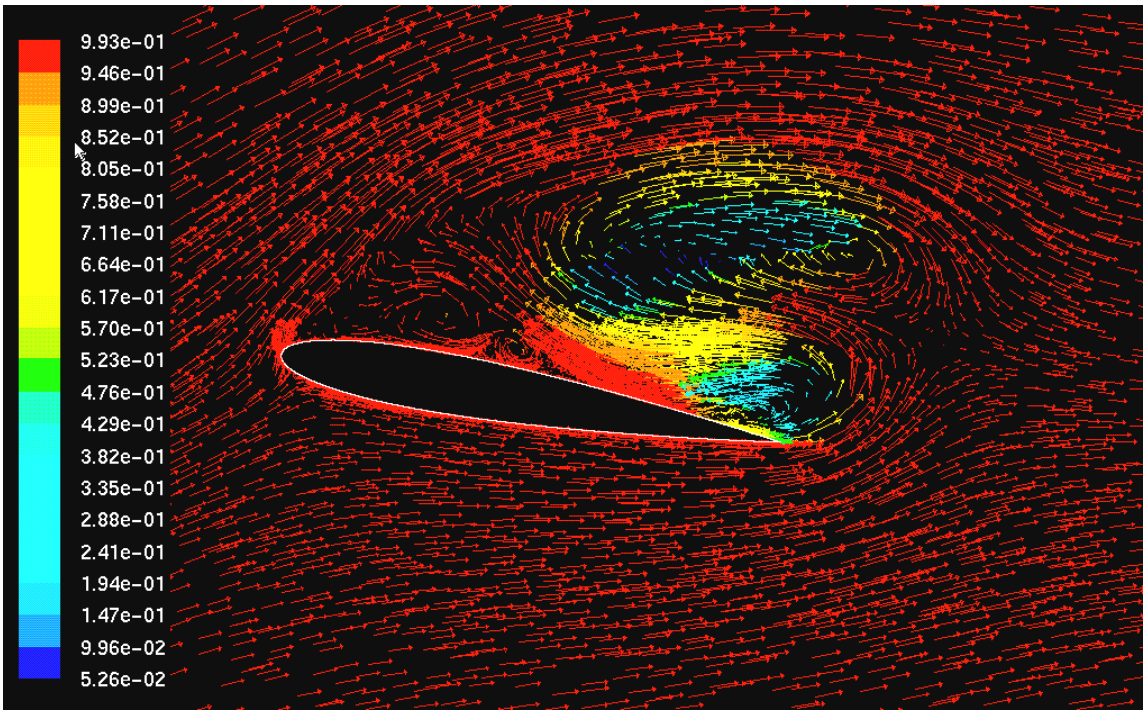

5.3 c) Angle = 24.95^{o}

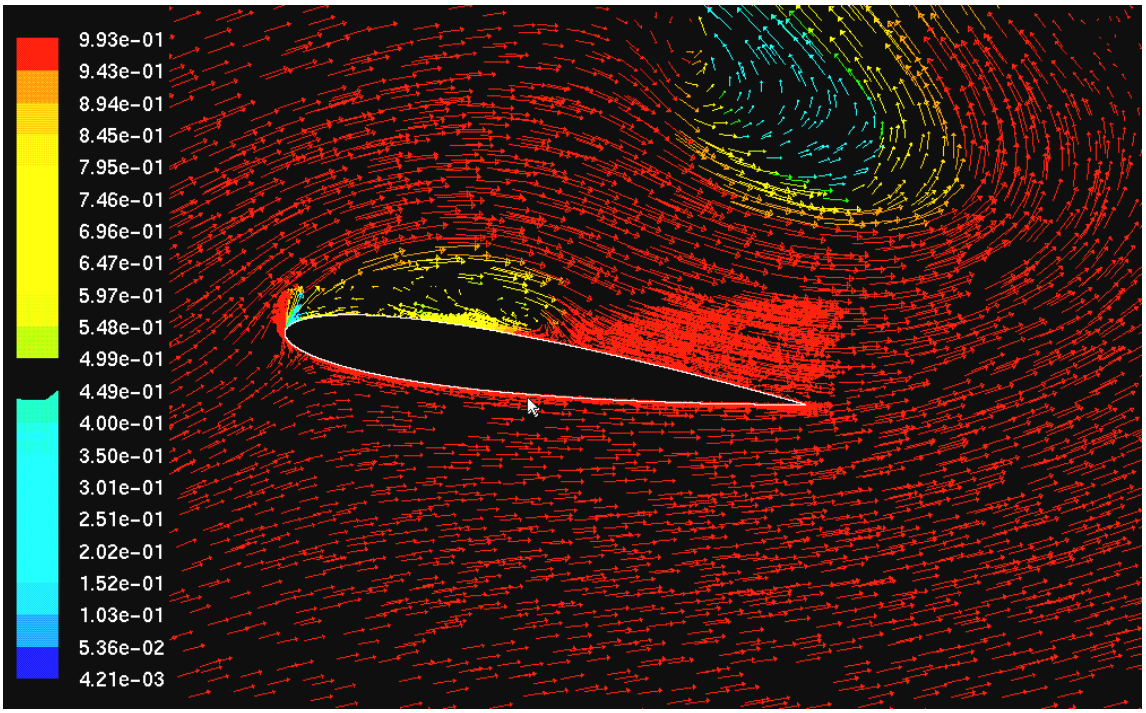

5.3 d) Angle = 24.23^{o}

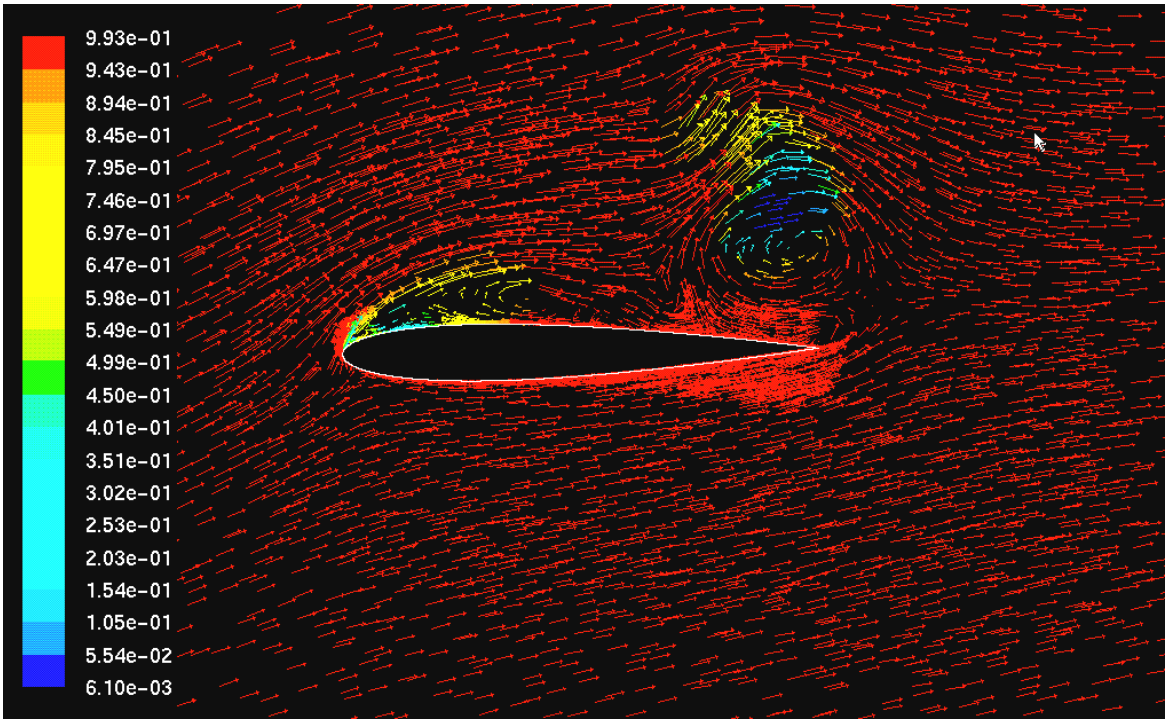

5.3 e) Angle = 21.24^{o}

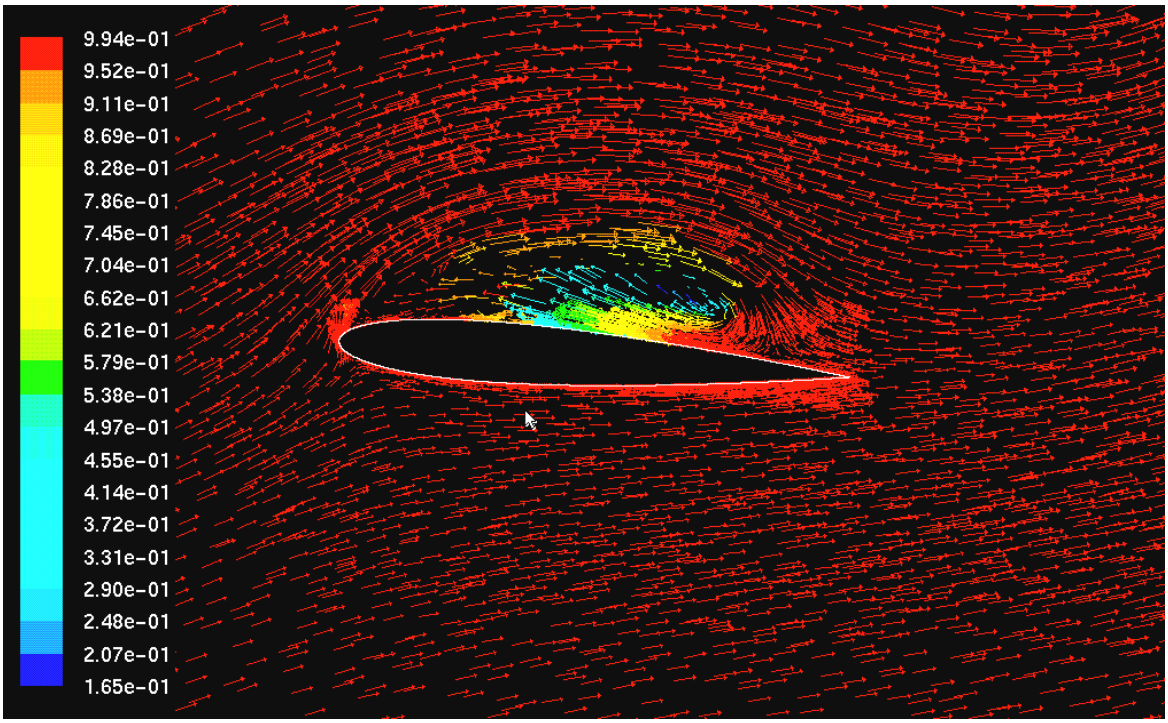

5.3 f) Angle = 11.8^{o}

Fig 5.3 Phase Contours showing the structure of Cavitation Clouds, k = 0.25, s = 2.7, Re = 10^{5}

5.1.3 Comparison of Coefficients of Lift and Drag for the cavitating and non-cavitating cases

The coefficients of lift and drag for the cavitating and non-cavitating cases are shown in Fig. 5.4. The considerable difference in the lift and drag curves, especially during the downward motion of the hydrofoil, indicate the impact of cavitation on the vortical flow structures of an oscillating hydrofoil. The large oscillations in lift and drag forces during the downward motion of the hydrofoil in the cavitating case are due to the increased strength of the secondary and tertiary vortices. The increase in the strength of these vortices is attributed to the early formation of these vortices in the oscillation cycle of the hydrofoil where by they have more time to develop and gain strength.

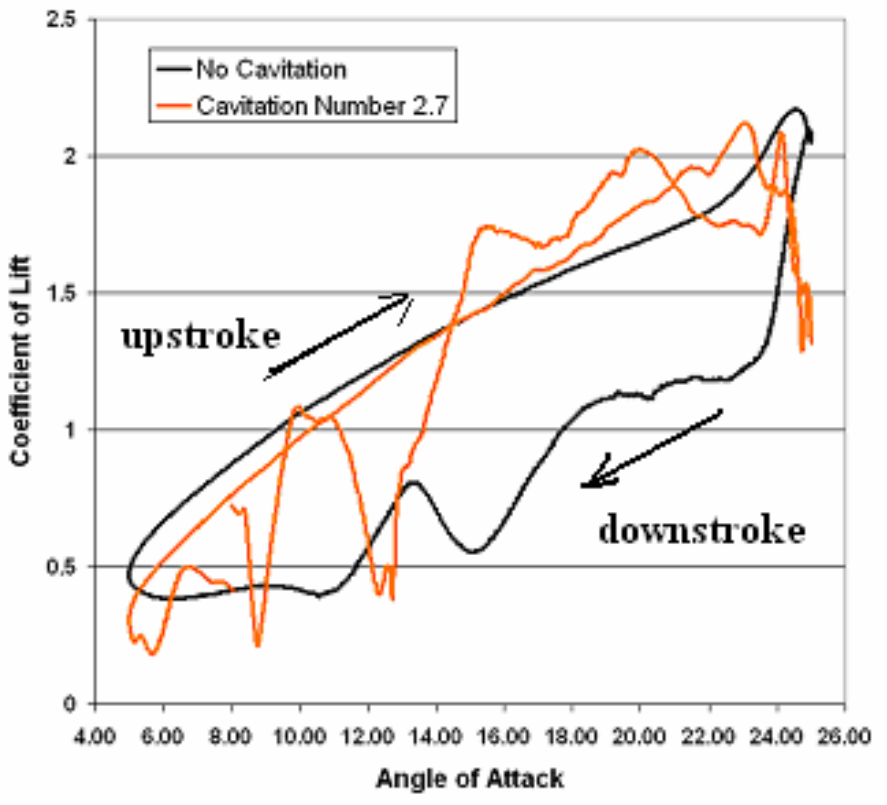

5.4 a) Comparison of Coefficient of Lift for the Cavitating and Non-cavitating case, k = 0.25, s = 2.7, Re = 10^5

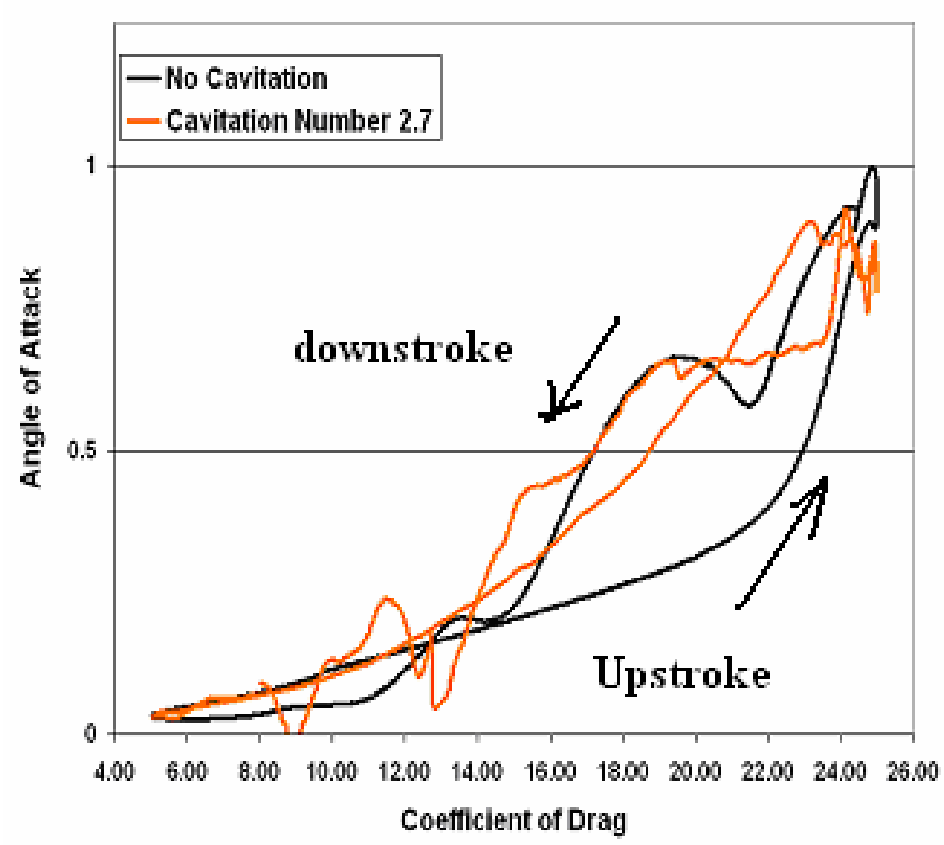

5.4 b) Comparison of Coefficient of Drag for the Cavitating and Non-cavitating case, k = 0.25, s = 2.7, Re = 10^5

5 .2 Oscillating Hydrofoil for Ship Stabilization

The validation studies indicated good agreement of the numerical simulation of non-cavitating large angle of attack oscillating hydrofoil with experimental results. Next, we use CFD to study the flow features of a hydrofoil oscillating from +28 degrees to -28 degrees. The behavior of the coefficient of lift is also studied as this is vital for a ship stabilization system.

Figure 5.5 shows the sequence of events as the hydrofoil oscillates sinusoidally. The mainstream flow is the horizontal direction. Figure 5.5a shows the hydrofoil at an angle of attack of -6^{o}, and pitching upwards. A separation zone can be seen on the bottom side of the hydrofoil. As the hydrofoil pitches upwards the flow gets completely attached and stays attached even at an angle of attack greater than the static stall angle as seen in Figure 5.5b. This is due to boundary layer stabilization effect brought about by 5the motion of the hydrofoil. Figure 5.5c shows the formation of dynamic stall vortex as well other secondary and tertiary vortex structures over the hydrofoil. As the hydrofoil reaches the maximum angle of attack and starts pitching downward, the primary dynamic stall vortex merges with a secondary vortex as seen in Figure 5.5d. As the hydrofoil moves down further and reaches angles of attack below static stall angle the flow gets fully attached as seen in Figure 5.5e. Figure 5.5f shows the hydrofoil pitching down and the flow separating at the bottom of the hydrofoil at angles of attack well above the static stall angle. This is due to the high pressure gradient on the suction side of the hydrofoil. Figure 5.5g, shows the hydrofoil pitching back up and the complex vortical flow structures can be seen on the suction side of the hydrofoil. The coefficient of Lift, drag and hydrodynamic moment on the hydrofoil is shown in the figure above. From the above discussion it is evident that the present CFD simulations capture complex vortical flow structure over an oscillating hydrofoil. The result obtained from the CFD simulation of sinusoidally oscillating hydrofoil is used in the mathematical model for active-fin ship stabilization system described above in the section of Fin/Hydrofoil dynamics.

Figure 5.6a shows the roll motion of ship without stabilization. The roll motion is seen to be as large as 15 degrees at the design condition of 5.5m significant wave height. Figure 5.6b shows the reduction in roll motion due to active fin ship stabilizer. The roll motion is seen to be constrained within 3 degrees which shows a considerable reduction.

Figure 5.7 shows the motion of hydrofoil in a typical ship stabilization system. The motion is seen to be closer to a trapezoidal motion. Presently, most studies on pitching airfoils/hydrofoils assume the motion to be sinusoidal, as they have been carried out for aerial rotor craft applications, whereas the motion of hydrofoils in a ship stabilization system will in general be non-sinusoidal. As the motion is significantly different from a sinusoidal motion an aerodynamic analysis of this motion will be conducted in the present study to see the lift, drag, and hydrodynamic moment behavior of the hydrofoil for this motion.

To keep the lift force under certain specified design conditions the angle of attack is kept within a certain maximum value. Presently to obtain high lift forces the hydrofoil is moved as quickly as possible to the maximum angle of attack. This is possible because the response time of the active-fin ship stabilization system is much smaller than the time period of roll motion. However if the hydrofoil is moved too quickly and maintained at the maximum angle of attack that is well above the static stall angle, we can expect a fall in lift forces due to separation. The high lift forces at these large angle of attack is mainly due to the pitching motion of the hydrofoil which stabilizes the boundary layer and

prevents separation, and the formation of the dynamic stall vortex near the leading edge whose passage further increases lift force.

Hence just maintaining the hydrofoil at max angle of attack will result in drop in lift force. Therefore it is desirable to find an optimum slew rate for the motion of fin, which will limit the amount of time the fin is maintained at the maximum angle of attack, and hence provide better performance. To examine this problem we have analyzed the motion of hydrofoil that is obtained from the system model of ship stabilizer described earlier. Figure 5.7 shows the variation of angle of attack with time. The motion of hydrofoil is seen to be closer to a trapezoidal motion. Figure 5.8 below shows the comparison between the hydrofoil motion and an equivalent sinusoidal motion. This motion generated from the system model developed for the entire ship stabilization system is fed to FLUENT for analysis of the hydrodynamic forces. The lift force generated by a trapezoidally oscillating hydrofoil is different than a sinusoidally oscillating hydrofoil. The lift generated by a large angle of attack oscillating hydrofoil depends on the motion of the hydrofoil. For the trapezoidal motion it is seen that during the period at which the hydrofoil is maintained at the maximum angle of attack of 28 degrees there is a considerable drop in lift force due to separation as the angle of attack is much higher than the static stall angle.

To understand the effect of pitch rate on the lift, drag and hydrodynamic moment, various motions for the hydrofoil were analyzed (Fig. 5.9). To find the best motion we can compare the time averaged lift force for half cycle (0-28-0 degrees). The highest time

averaged coefficient of lift was obtained for the sinusoidal motion as seen from table 5.1. For the trapezoidal motion there was a slight drop in time-averaged coefficient of lift. Also as the pitch rate was increased from 14.9 deg/s to 23 deg/s there was a drop in the time averaged lift force. and 22% increase in drag force, while the hydrodynamic moment was nearly constant. The higher time-averaged drag force would result in higher propulsion power requirement for the ship. This clearly shows that increase in pitch rate can lead to decrease in lift force and increase in drag force and hence the pitch rate needs to be controlled.

The high drag force experienced by the oscillating hydrofoil is due to the passage of dynamic stall vortex over the suction side of the hydrofoil. At higher pitch rates (23 deg/s) the passage of dynamic stall vortex takes place early in the cycle and the hydrofoil is then maintained at the max angle of attack for a longer time. When the hydrofoil is maintained at maximum angle of attack large drag force persist due to separation. It is also seen that with higher pitch rates the maximum value of lift force is lower. This is due to the time-lag effects. When the hydrofoil is pitching the flow will take certain amount of time to adjust to the new angle of attack. As the hydrofoil is pitching faster the phase lag between the flow and the angle of attack is higher hence lower lift forces are generated at max angle of attack (28 degrees). The oscillations seen in lift force for trapezoidal motion is due to oscillations in the angular velocity (obtained from system model) when the hydrofoil reaches the max angle of attack.

Table 5.1: Time Averaged Coefficient of Lift, Drag and Moment

No.	Motion	Time Averaged Coefficient of Lift for Half Cycle	Time Averaged Coefficient of Drag for Half Cycle	Time Averaged Coefficient of Moment for Half Cycle
1	Sinusoidal	1.15	0.412	0.174
2	Trapezoidal (Pitch Rate =14.9 deg/s)	1.09	0.356	0.130
3	Trapezoidal (Pitch Rate = 23 deg/s)	1.06	0.436	0.131

Table 5.2: Time Averaged Coefficient of Lift, Drag and Moment as percentage of values from sinusoidal motion

No	Motion	Time Averaged Coefficient of Lift (Percentage of Lift from Sinusoidal Motion)	Time Averaged Coefficient of Drag (Percentage of Drag From Sinusoidal Motion)	Time Averaged Coefficient of Moment (Percentage of Moment from Sinusoidal Motion)
1	Sinusoidal	100%	100%	100%
2	Trapezoidal (Pitch Rate =14.9 deg/s)	94.8%	86.4%	74.7%
3	Trapezoidal (Pitch Rate = 23 deg/s)	92.2%	105.8%	75.2%

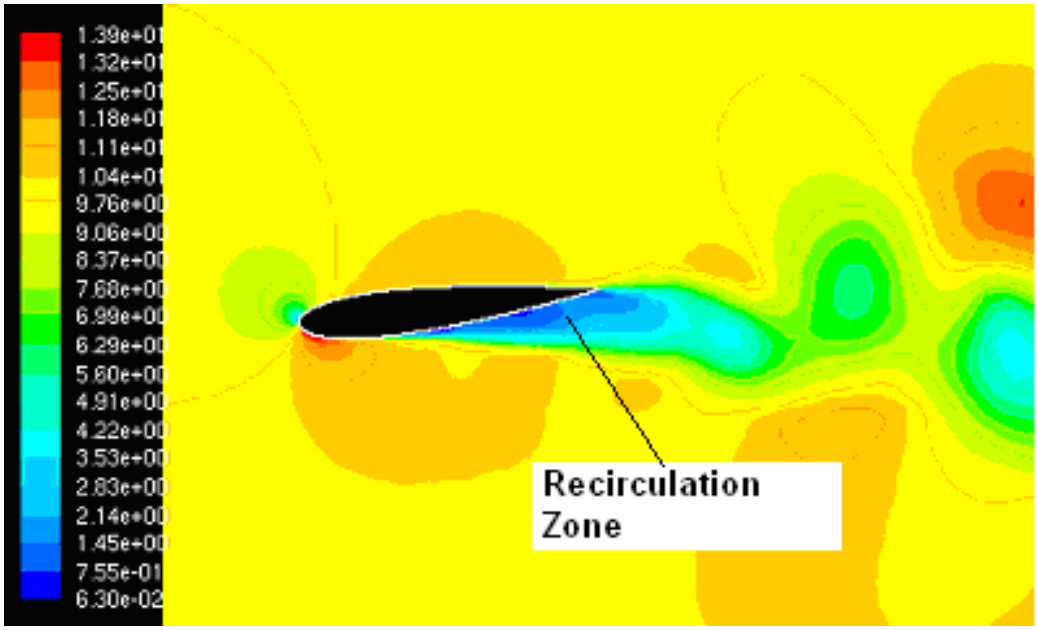

5.5a) Angle = -6 degrees (Pitch Up)

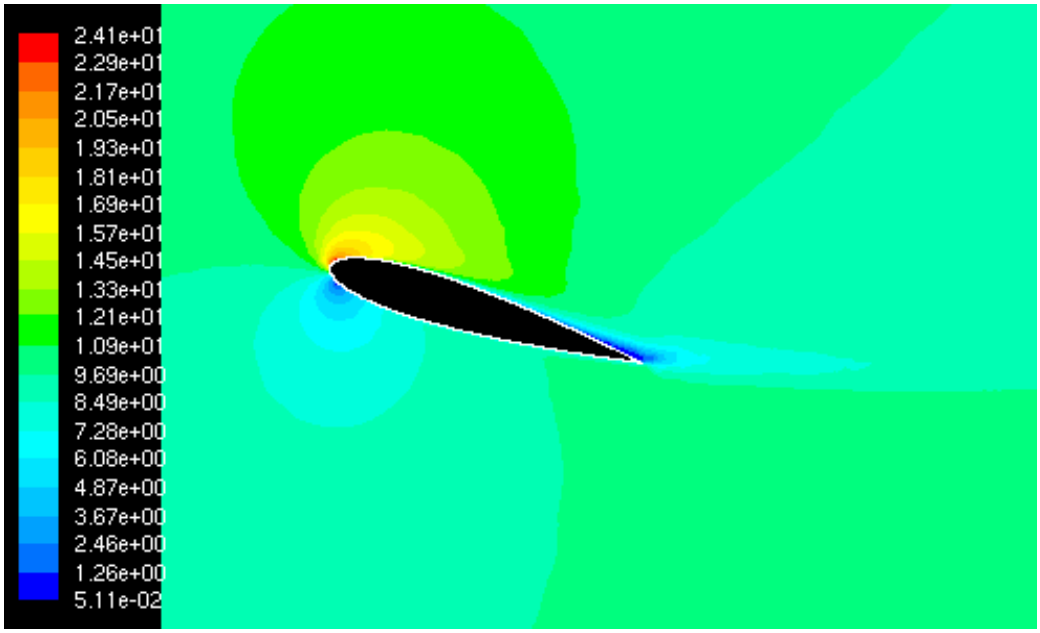

5.5b) Angle = 17.5 degrees (Pitch Up)

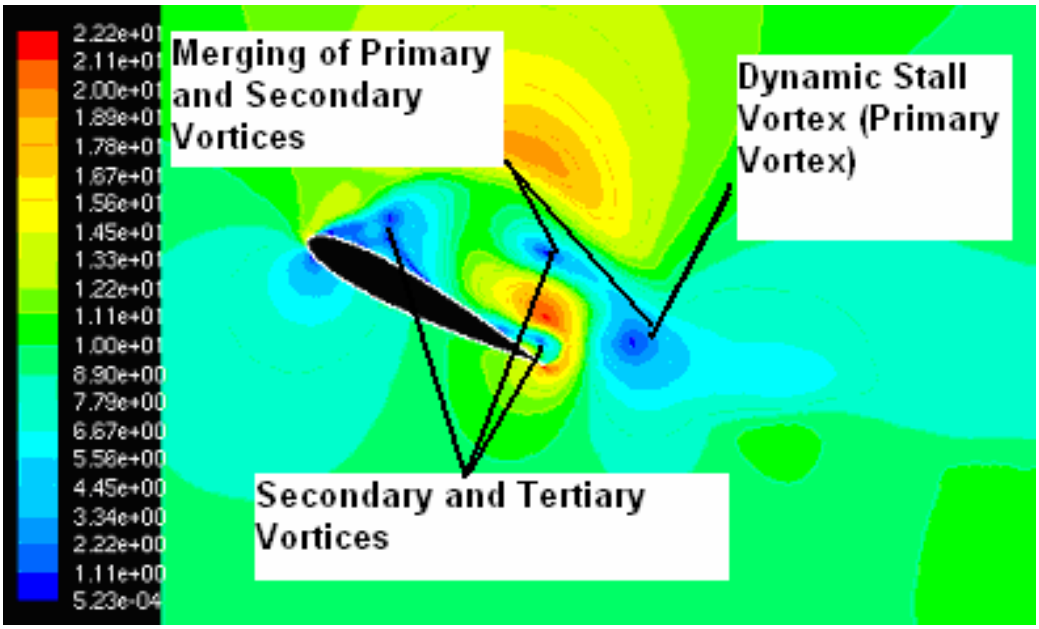

5.5c) Angle = 28 degrees (Max Angle of Attack)

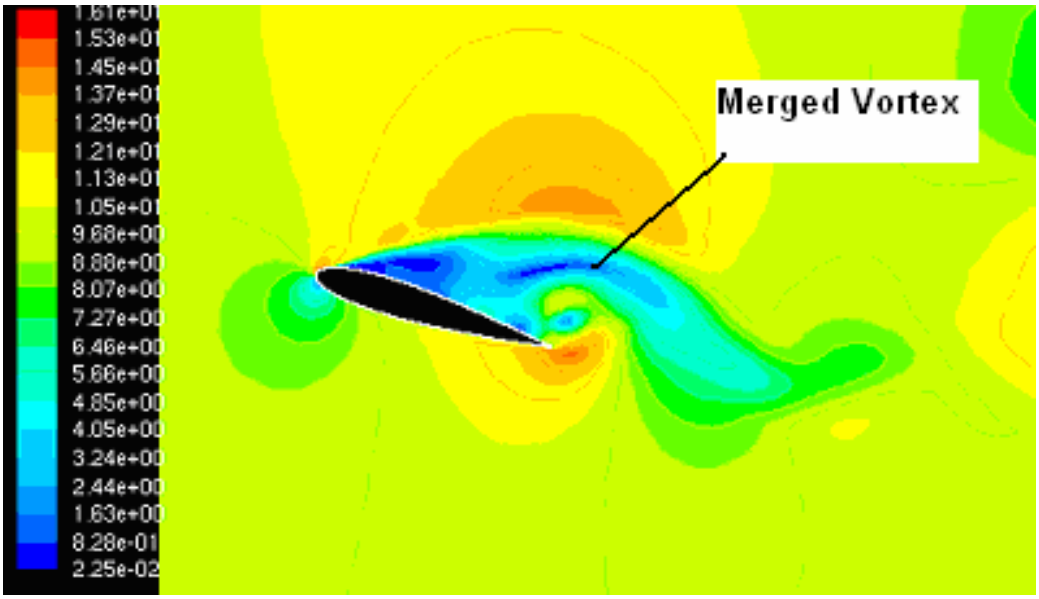

5.5d) Angle=17.52 (Pitch Down)

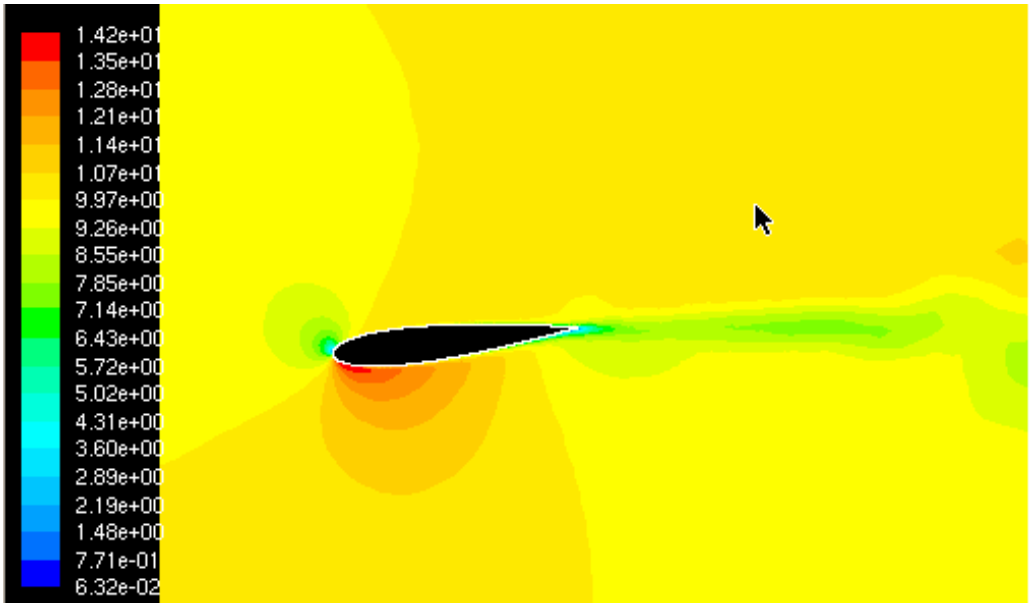

5.5e) Angle = - 6.2 (Pitch Down)

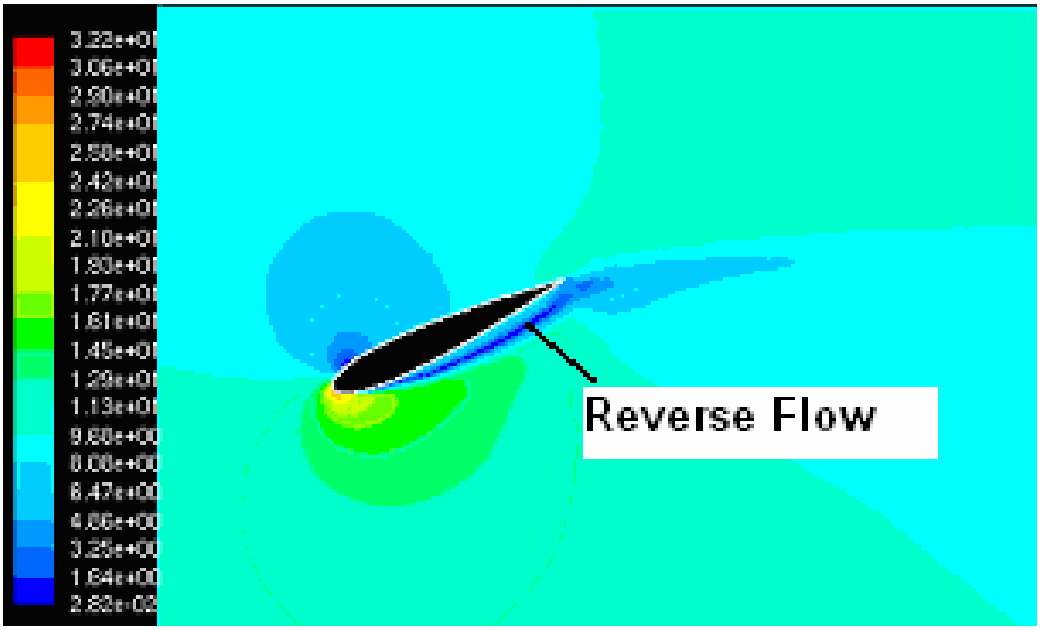

5.5f) Angle = - 25.25 (Pitch Down)

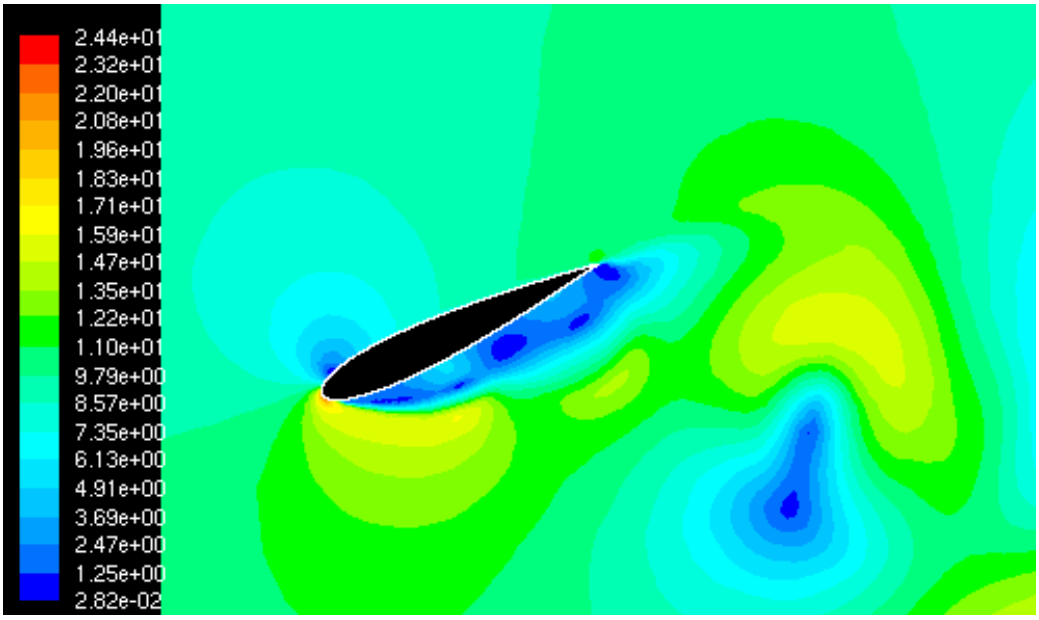

5.5g) Angle = -25.2 (Pitch Up)

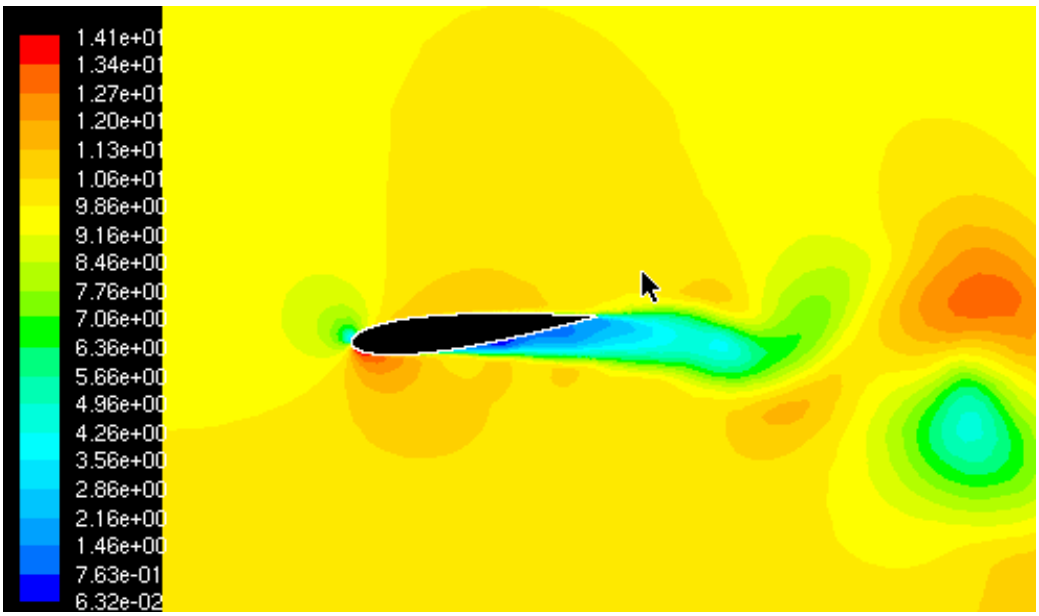

5.5h) Angle = -6.12 (Pitch Up)

Fig 5.5 Velocity Contours, Non-cavitating 0-28-0—28-0,, k = 0.08, Re = 10^6

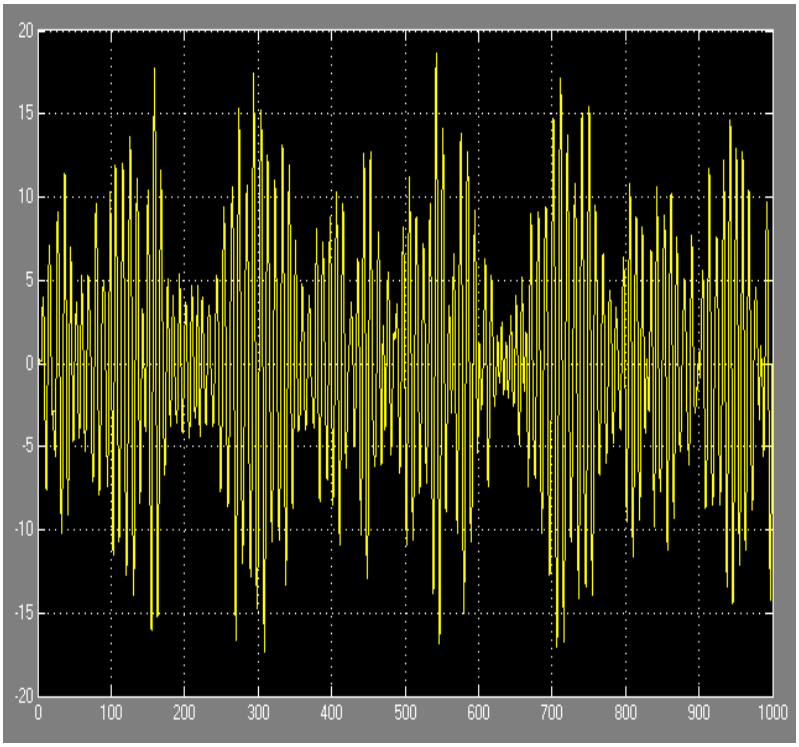

Fig 5.6 a) Unstabilized Roll angle in Degrees vs Time, H1/3=5.5m

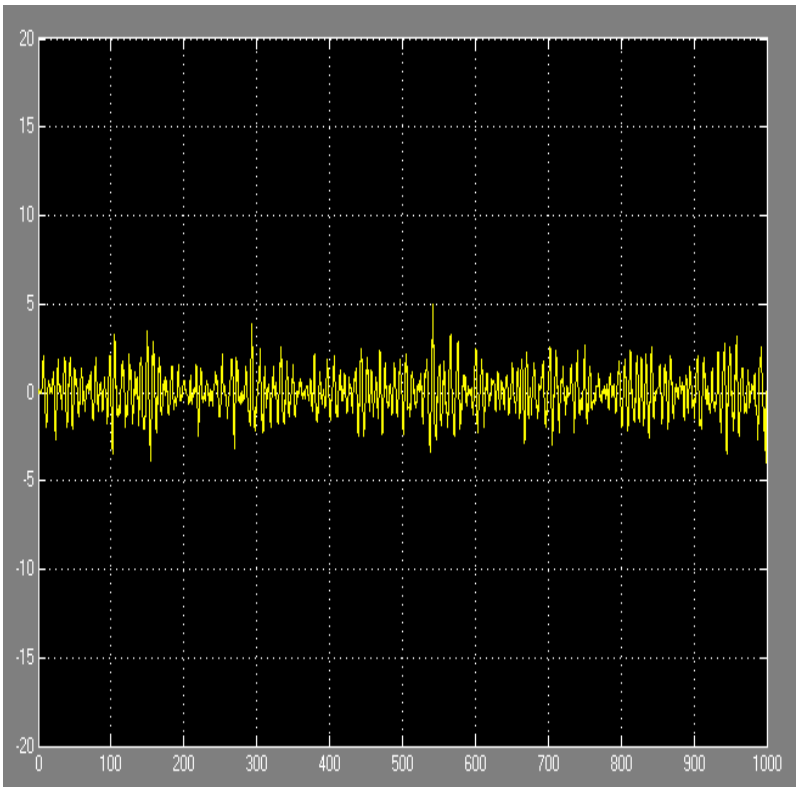

Fig 5.6 b) Unstabilized Roll angle in Degrees vs Time, $H_{1/3}$=5.5m

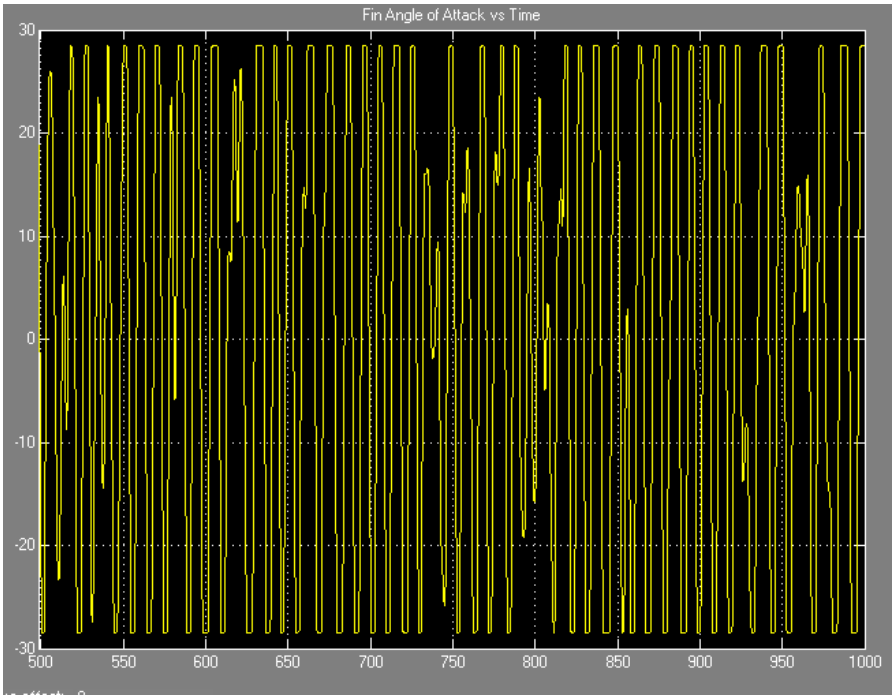

Fig 5.7 Fin angle of attack in Degrees vs Time

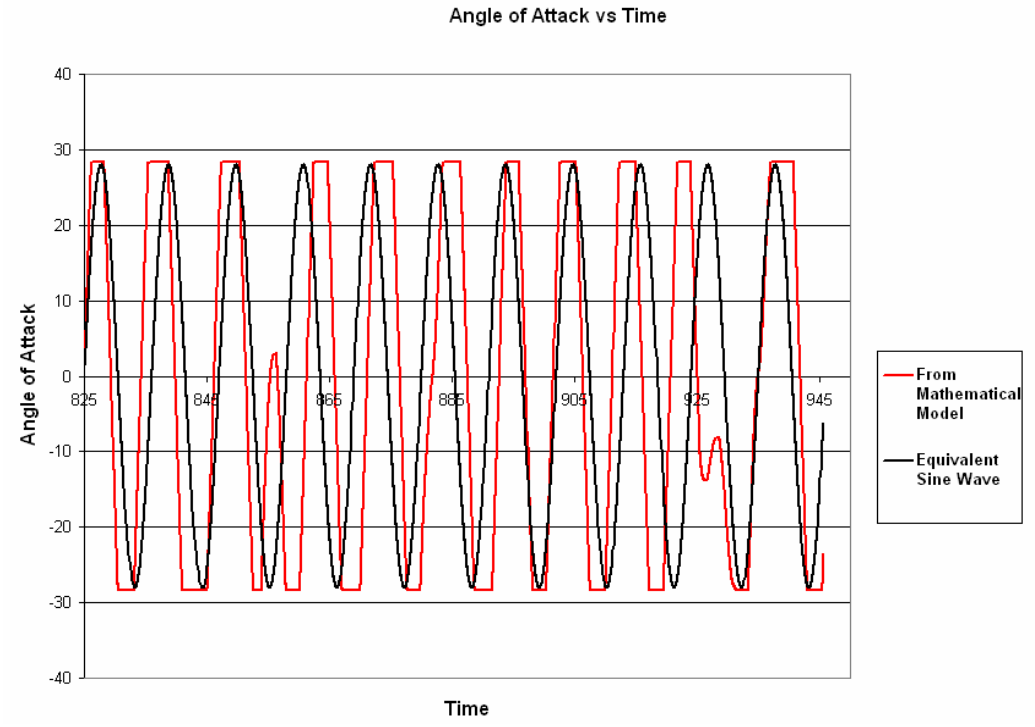

Fig 5.8 Fin angle of attack in Degrees vs ExpandedTime

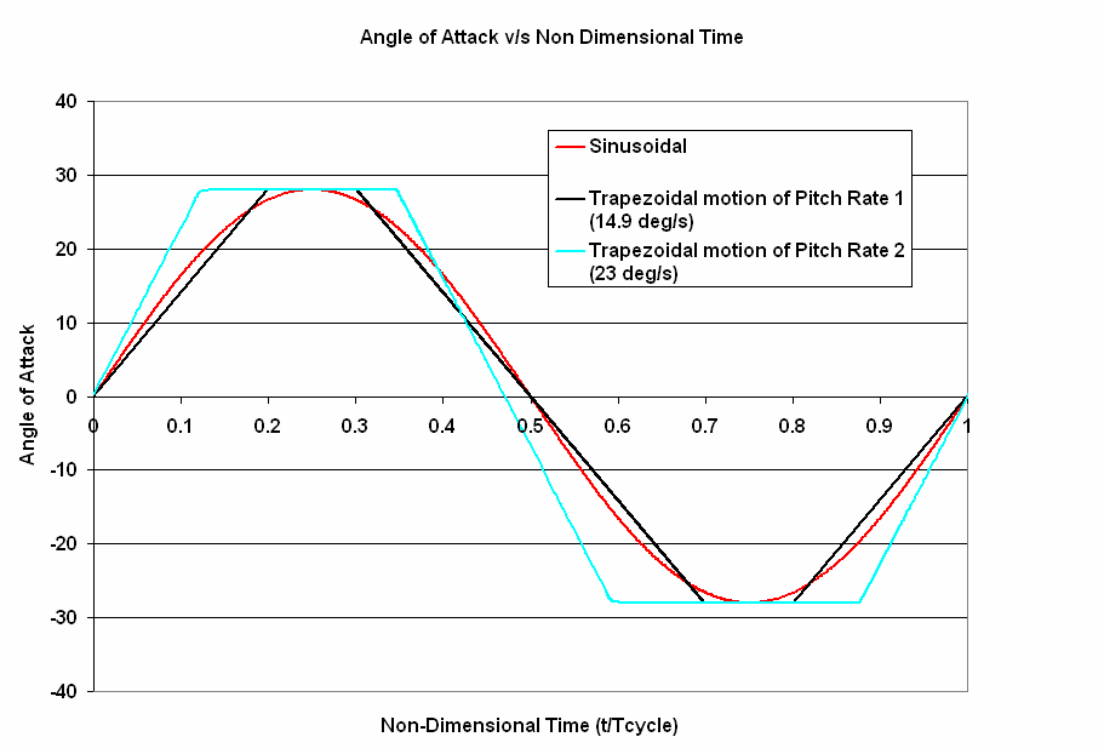

Fig 5.9 Angle of Attack vs Non Dimensional Time (t/T_{cycle})

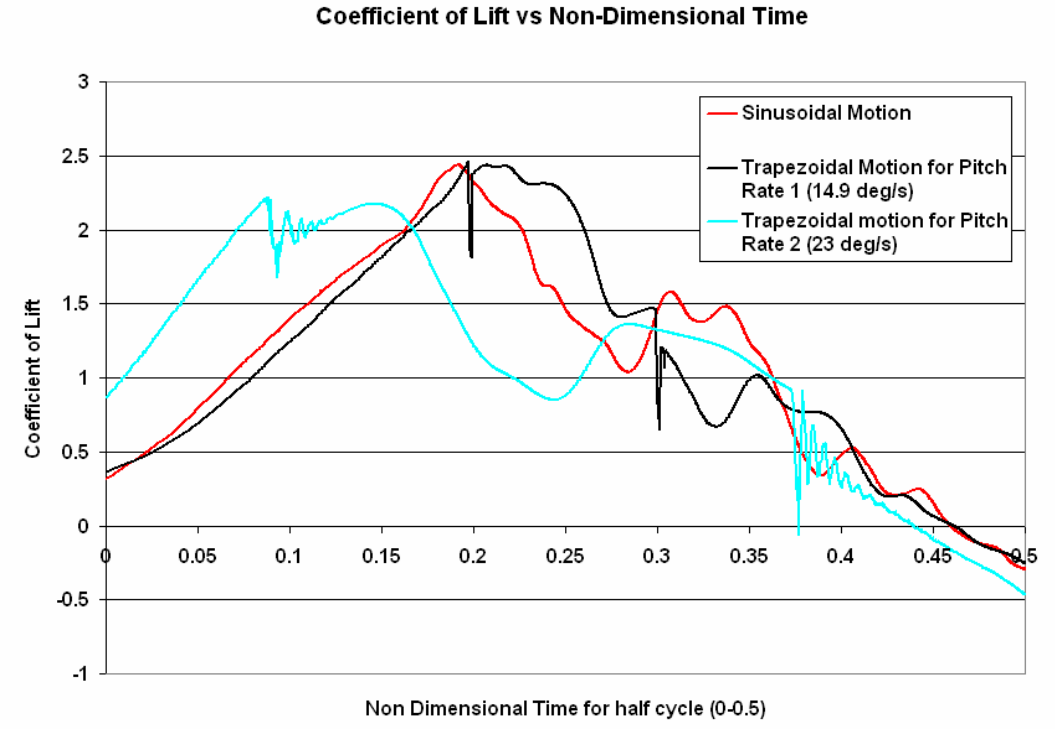

Fig 5.10 Coefficient of Lift of Hydrofoil vs Non Dimensional Time (t/Tcycle)

Chapter 6 Conclusion and Future Work

This chapter presents the conclusions obtained from the present study and provides direction for the future work.

6 .1 Conclusion

Cavitation considerably influences the physics of the flow over an oscillating hydrofoil. Cavitation resulted in early formation of the dynamic stall vortex because of the expansion of separation bubble existing near the suction peak of the hydrofoil. The strength of the dynamic stall vortex is reduced because of vapor formation, which limits the lower pressure to the vapor pressure in the core. The vortical flow structures are highly distorted as the vortex core expands due to vapor formation. The pairing of vortices 'B' and 'D' was not observed because of their lower strength which can be attributed to the lower strength of dynamic stall vortex. Additional vortices 'E' and 'F' are observed. The large fluctuations of coefficient of lift during the down stroke indicate higher strength of tertiary and quaternary vortices. This is because of higher vorticity concentration in these regions as a result of cavitation. Good correlation was observed between the formation, convection and dissipation of vortical flow structures and the variation of coefficient of lift and drag.

CFD has been used for study of active-fin ship stabilization system and to predict its performance. A mathematical model has also been developed to simulate the entire ship stabilization system. The active-fin ship stabilizer is seen to capable of limiting the roll motion significantly at design conditions.

Aerodynamics of the trapezoidally moving hydrofoil was investigated to find out the effect of pitch rate of the hydrofoil on the lift, drag and moment of the hydrofoil. It was found that at higher pitch rates there was a reduction in lift forces and considerable increase in the drag force. Also the percentage drop in lift force for trapezoidal motion was much less than the drop in hydrodynamic moment as compared with the sinusoidal motion. Since hydrodynamic moment is the major opposition to the pitching motion of the hydrofoil, lower moment would mean lower power requirements for operating the stabilizer.

6 .2 Future Work

As a part of future study we will examine effect of change in cavitation number and reduced frequency on the vortex dynamics of oscillating hydrofoil. Simulations of three-dimensional hydrofoil will be carried out to study the effect of span wise instabilities on the vortex dynamics and interaction of tip vortex with the dynamic stall vortex. Improvements in the system modeling process by coupling the CFD software Fluent with MATLAB will help to simulate the system more accurately. This will be carried out as a part of future analysis.

.

References

Arandt, R.E.A., Kjeldsen, M., Song C, C, S., and Keller, A., (2000) "Instability of Partial Cavitation: Numerical/Experimental Approach," 23rd Symposium on Naval Hydrodynamics.

Astolfi, J, A, (2001), " An Experimental Investigation of Partial Cavitation on a Two - Dimensional Hydrofoil", CAV 2001: Fourth International Symposium on Cavitation, June 20-23, California Institute of Technology, Pasadena, CA USA.

Belahadji, B., Franc, J, P., and Michel, J. M., (1995), "Cavitation in the Rotational Structures of a Turbulent wake," Journal of Fluid Mechanics, Vol. 287, pp. 383-403.

Caron, J, F., Farhat, M., Avellan, F., (2000), "On the Leading Edge Cavity Development of an Oscillating Hydrofoil", Proceedings of the ASME Fluids Engineering Division Summer Meeting, Boston, Massachusetts, USA.

Chen, Y., Heister S, D., (1994), "A Numerical Treatment for Attached Cavitation", Journal of Fluids Engineering, V116, pp 613-618.

Coutier-Delgosha, O., Fortes-Patella, R., and Reboud, F., (2001) "Evaluation of the Turbulence Model Influence on the Numerical Simulation of Unsteady Cavitation," ASME Fluids Engineering Division Summer Meeting.

Delannoy, Y.,, Kueny J, L., (1990), "Two phase flow approach in unsteady cavitation modeling", Cavitation and Multiphase Flow Forum.

Ekaterinaris, J. A. (1995), "Numerical investigation of dynamic stall of an oscillating wing". AIAA J. 33(10), 1803-1808.

Erricson L. E. and Reding J. P. (1976), "Dynamic stall analysis in light of recent numerical and experimental results" J. Aircraft 248-255.

Erricson L. E. and Reding J. P. (1979), ”Dynamic stall at high frequency and large amplitude" J. Aircraft 136-142.

Erricson L. E. and Reding J. P. (1984), “Unsteady flow concepts for Dynamic stall analysis” J. Aircraft 601-606.

Erricson L. E. and Reding J. P. (1988), "Fluid mechanics od dynamic stall Part I Unsteady flow concepts" J. Fluids and Structures, 2,1-33.

Fortuna, L. and Muscato, G., (1996), "A Roll Stabilization System for a Monohull Ship: Modeling, Identificcation, and Adaptive Control," IEEE Transactions on control systems technology, Vol. 4, No 1.

Furness, R. A.; Hutton, S. P., (1975), “Experimental and theoretical studies of two-dimensional fixed-type cavities”, Journal of Fluids Engineering, vol. 97, Dec. 1975, p. 515-521

Gangwani, S. T. (1982) “Prediction of dynamic stall and unsteady airloads for rotor blades,”. J. Amer. Helicopter Soc. 57-64.

Ghia, K. N., Yang, J. Oswald, G. A. and Ghia, U. (1991), ”Study of dynamic stall mechanism using simulation of two-dimensional Navier-Stokes equations”, AIAA Paper, 91-0546.

Ghia, K. N., Yang, Y., Oswald, G. A. and Ghia, U. (1992), ”Study of the role of unsteady separation in the formation of dynamic stall vortex”. AIAA Paper 92-0196.

Guilmineau, E., Piquet, J., and Queutey, P., (1997) "Unsteady Two Dimensional Turbulent Viscous Flow Past Aerofoils," International Journal for Numerical Methods in Fluids, Vol. 25, 1997, pp. 315-366.

Guo, C. and Sun, Z., "Neuro-Fuzzy Intelligent Controller for Ship Roll Motion Stabilization," Proceedings of the 2003 IEEE International Symposium on Intelligent Control, Vol. 4, No 1, 1996.

Hickey, N, A., Grimble, M, J., Johnson, M, A., Katebi, M, R., and Melville, R.," Robust Fin Roll Stabilization of Surface Ships," Proceedings of 36th conference on decision and control, 1997.

Fung, K. Y. and Carr, L. W. (1991) Effects of compressibility on dynamic stall. AIAA J. 26(2), 306-308.

Halfman, R. L., Johnson, H. C. and Haley, S. M. (1951) “Evaluation of high-angle-of attack aerodynamic derivative data and stall flutter prediction techniques”. NACA TN 2533.

Kawanami, Y; Kato, H; Yamaguchi, H; Tanimura, M; Tagaya, Y, (1997) Mechanism and control of cloud cavitation, Journal of Fluids Engineering, Transactions of the ASME. Vol. 119, no. 4, pp. 788-794.

Kjeldsen, M., Arndt, R, E, A., Effertz, M., (1999), Investigation of unsteady cavitation phenomenon, Proc. ASME Cavitation and Multiphase Flow Forum.

Kubota, A., Kato, H. And Yamaguchi, H.,1992, "A New Modelling of Cavitation Flows: A Numerical Study of Unsteady Cavitation on a Hydrofoil Section," Journal of Fluids Mechanic, 240, 59-96.

Laberteaux, K., Ceccio, S, L., (1998), Partial attached cavitation on two-and three-dimensional hydrofoils, Proc. 22nd ONR Symp. on Naval Hydrodynamics.

Landon, R. H. (1982) "NACA-0012 oscillatory and transient pitching," AGARD Report 702.

Lorber, P. F. (1992) Compressibility effects on the dynamic stall of a three-dimensional wing, AIAA Paper 92-0191.

Lush, PA, Peters PI (1982), Visualisation of the cavitating flow in a Venturi-type duct using high speed cine photography, Proc. IAHR Conf. on Operating Problems of Pump Stations.

McAlister, K, W., Pucci, W, J., McCrosky, W, J., and Carr, W, L., (1982) "An Experimental Study of Dynamic Stall on Advanced Aerofoil sections. Pressure and Force data," NASA TM 84245.

Mehta, U. B. (1977) Dynamics stall of an oscillating airfoil, AGARD CP 227, Paper No. 23, 1-32.

Newsome, R. W. (1994) Navier-Stokes simulation of wing-tip and wing-juncture interaction for a pitching wing. AIAA Paper, 94-2259.

Pham, T, M., Larrarte, F., Fruman, D, H., (1999) Investigation of Unstable Sheet Cavitation an Cloud Cavitation Mechanisms, ASME J. Fluids Eng.

Piziali, R. A. (1993) “An experimental investigation of 2D and 3D oscillating wing aerodynamics for a range of angle of attack including stall,” NASA Technical Memorandum 4632.

Qin, Q., Song, C, S., and Arndt, R, E, A., "A Numerical Study of an Unsteady Turbulent Wake Behind a Cavitating Hydrofoil," Fifth International Symposium on Cavitation, 2003.

Raffel, M., Kompenhaus, J., and Wernert, P., (1995) "Investigation of the Unsteady Floe Velocity Field Above an Aerofoil Pitching in deep Dynamic Conditions," Exp Fluids, Vol. 19, 1995, pp. 103-111.

Rumsey, C. L. and Anderson, W. K. (1988) Some numerical and physical aspects of unsteady Navier-Stokes computations over airfoils using dynamics meshes. AIAA Paper 88-0329.

Sankar, L. N. and Tassa, W. (1981) Compressibility effects of dynamic stall of a NACA-0012 airfoil. AIAA J. 19(5), 557-568.

Sankar, L. N. and Tung, W. (1985) Numerical solution of unsteady viscous ßow past rotor sections. AIAA Paper 85-0129.

Singhal, A, K., Athavale M, M., Li, H., and Jiang, Y., "A Mathematical Basis for Validation of Full Cavitation Model," Journal of Fluids Engineering, Vol. 124, 2002, pp. 617-624.

Song, C, He, J., (1998), “Numerical simulation of cavitating flows by single-phase flow approach”, Third International Symposium on Cavitation.

Sridhar, G., Katz, J., "Effect of entrained bubbles on the structure of vortex rings," Journal of Fluid Mechanics, Vol. 397, 1999, pp. 171-202.

Srinivasan, G. R., Ekaterinaris, J. A. and McCroskey, W. J. (1995) Dynamic stall of an oscillating wing, Part 1: Evaluation of turbulence models. Comput. Fluids 24(7), 833-861.

Stutz, B. and Reboud, J.L., 1997, "Experiment on Unsteady Cavitation," Exp. Fluids, 22, 191-198.

McCroskey, W. J. (1981) “The phenomenon of dynamic stall,” NASA TM-81264.

Xing, T., Zhenyin, L., Frankel, S, H., "Effect of Cavitation on Vortex Dynamics in a Submerged laminar Jet," AIAA Journal, Vol. 40, No. 11, Nov. 2002.